



IMPACT OF GEOGRAPHICAL INFORMATION SYSTEMS ON GEOTECHNICAL ENGINEERING

J. David Rogers & Ronaldo Luna

University of Missouri – Rolla

Rolla, Missouri – USA – 65401

ABSTRACT

Over the last four decades Geographical Information Systems (GIS) have emerged as the predominant medium for graphic representation of geospatial data, including geotechnical, geologic and hydrologic information routinely used by geotechnical and geoenvironmental engineers. GIS allow unlimited forms of spatial data to be co-mingled, weighted and sorted with any number of physical or environmental factors. These data can also be combined with weighted political and aesthetic values to create hybrid graphic products capable of swaying public perceptions and decision making. The downside of some GIS products is that their apparent efficacy and crispness can also be deceptive, if data of unparalleled reliability is absorbed in the mix. Disparities in data age and quality are common when compiling geotechnical and geoenvironmental data. Despite these inherent shortcomings, GIS will continue to grow and evolve as the principal technical communication medium over the foreseeable future and engineers will be forced to prepare their work products in GIS formats which can be widely disseminated through the world wide web. This paper presents the historical evolution of GIS technologies as it relates to the impact in geotechnical engineering, concluding with four case histories on the application of this emerging technology.

INTRODUCTION AND BACKGROUND

Origins of Remote Sensing

In 1904 the U.S. Geological Survey began using terrestrial photogrammetry to aid its topographical mapping of remote mountainous regions in Alaska. In 1907 German inventor Alfred Maul began placing gyroscopically stabilized Rolliflex cameras in rockets. By 1912 his system was able to propel a 41 kg payload to altitudes of 2600 feet to make aerial oblique images. The first aerial photo imaged from a manned aircraft in the United States was in November 1910, when Orville Wright took a newspaper photographer aloft near what is now Wright-Patterson AFB.

During the First World War (1914-18) aerial photography became a commonplace tool for military reconnaissance, initially limited to observation of enemy positions and movements. Both sides soon learned that aerial images could be exploited to discern remarkable detail about military conditions and disbursements, and this discovery naturally led to the rapid development of camouflage and concealment techniques that had been unimaginable a few years previous. Development of sophisticated aerial cameras began during the war, with the first multiple lens aerial cameras being developed by the USGS in 1916. Between 1918-20 Sherman Fairchild developed an aerial camera with a focal plane shutter, which became the industry standard for several decades thereafter. In 1924 Fairchild completed an exquisite map of New York's five boroughs with sufficient resolution to discern individual cars on Fifth Avenue and summertime crowds on Coney Island (Brandt, 1990).

The 1920s saw the emergence of aerial mapping as a significant engineering tool, beginning with the U.S. Geological Survey (USGS) mapping of Santo Domingo and Haiti in 1920. The first topographic map derived from aerial imagery appeared the following year (Reelfoot Lake quadrangle in Tennessee-Missouri-Kentucky). Aerial photos began to be used for timber inventory purposes in 1923, for railroad alignments in heavily forested areas in 1924, for locating highways and tunnels as early as 1924, for petroleum exploration and geologic mapping by 1926, and route surveying for locating pipelines and transmission lines by 1929. The stereo-autograph was developed in Germany and initially brought to America by the USGS in 1924. By 1927 the USGS had developed a protocol using stereophotogrammetry to create topographic maps, and this technology gradually eclipsed plane tabling as the primary means of map construction over the succeeding decade, using their Multiplex Aeroprojector. The U.S. Soil Conservation Service instituted a nationwide program to inventory soils in beginning in 1933, which succeeded in covering the continental 48 states and territories by 1941.

After the Second World War the USGS began to photograph the continental United States to develop 7.5 minute (1:24,000 scale) and 15-minute (1:62,500 scale) orthophoto-derived topographic maps. This first generation of photos were imaged between 1946-49, and the initial series of 7.5-min. maps were released between 1947-59. Less inhabited regions, such as mountains and forests, were covered by the larger scale 15-minute maps. In 1956 the USGS began imaging a second series of aerial photos across the metropolitan areas experiencing rapid post-war growth, such as portions of New York, Texas and California.

This was part of a program then envisioned library photography on 10-year intervals. The “second generation” of 7.5 minute maps began being released in the late 1950s, based on successive imagery. Contour intervals were generally 10, 20 or 40 feet on the 7.5 minute series maps and 20, 40 or 80 feet on the 15 minute series maps.

In the early 1970s the USGS committed to mapping all of the continental United States and Hawaii on 7.5-minute 1:24,000 scale maps. This program was completed in September 1990. Since 1991 Digital Raster Graphic (DRG) overlays have been selectively produced of areas experiencing rapid urban growth. The new DRGs use gray shadowing without replicating any changes to the topography caused by mass grading. These updates are electronically generated overlays developed from aerial imagery. Funding for USGS mapping activities was severely curtailed during the 106th Congress in 1994, and hard copy map products are gradually being withdrawn from circulation in favor of digital map products, such as DRGs, Digital Orthophoto Quarter Quadrangles (DOQQs), Digital Line Graphics (DLGs) and other specialized products, such as the nation’s largest cities being profiled in The National Map program. Most of these are available on the Internet or in electronic format, on CD-ROM.

Modern remote sensing as we know it today, using digital imaging, evolved from development work by the military and NASA. In May 1960 CIA pilot Francis Gary Powers U-2 spy plane was shot down over the central Soviet Union, ending conventional over flights to obtain photo intelligence in the visible light spectrum. The military turned to NASA to help develop camera-equipped satellites and more capable aircraft that could be used to gather information above high threat areas without the risk of being shot down. In 1960 NASA launched Tiros-1, a meteorological satellite. Tiros showed “indications that space technology would someday have a significant role to play in obtaining information to better measure, map, monitor, model, and manage Earth’s finite resources” (Estes, et al, 1980).

In 1972 NASA launched Landsat-1 and this changed the way mankind viewed the planet. The Landsat program launched five satellites carrying a variety of remote sensing systems designed to acquire different kinds of Earth resource information. The Landsat program was crucial for the development of GIS because the remotely sensed geographic information was imaged and distributed in a digital format. This precluded the need for time-consuming manual encoding of data which had been the bane of the Harvard Lab graduate students since its inception. With this information, GIS users have been able to use satellite imagery, either in spatial or spectral resolution, to conduct everyday business and research since 1972.

Origins of GIS

A parallel, but no less significant development during this same period was the establishment of the fledging field of urban planning, influenced by Frederick Law Olmstead, who had designed New York’s Central Park in 1874. Planners saw the potential for using aerial photography and maps as their principal

form of communicating spatial information, and found it especially effective for illustrating the contrasts between developed and undeveloped landscape, which would rise to the forefront of the national consciousness in the decade between 1965-75.

In the early part of the 20th Century allied disciplines began using topographic and cadastral maps as spatial information datums, and thereby converted maps into spatial databases. Some early examples would be: 1) weather data maps; 2) variation in measured ocean currents by month of the year; and 3) surface runoff volumes, which were manipulated graphically to exhibit the relative differences in flow volume between channels. Much of this data was crucial to navigation/commerce and agriculture. By 1912 the overlay of multiple spatial themes was introduced in some planning studies for burgeoning business centers such as New York, Philadelphia and Boston.

The multifaceted aspects of the emerging field of urban planning more or less culminated in the release of the "*Town and Country Planning Textbook*" in Great Britain five years after World War II (Association for Planning and Regional Reconstruction, 1950). This volume became a post-war blueprint for the aesthetic layout of urban suburbs beyond the established business and commercial districts, with mass transit systems moving people between work and home. Much of the stimulus for this movement was to avoid overcrowding that had come to typify the great business centers, like London and New York City.

In the late 1950s Canadian scientists Roger Tomlinson saw the need for computers to perform certain simple but enormously labor-intensive tasks associated with the Canada Land Inventory. This computerized inventory, known as Canada-GIS (CGIS) appeared in 1964. Most texts credit it with being the first true Geographical Information System (GIS).

Around 1965 Professor Edgar Horwood of the University of Washington and Howard Fisher at Harvard combined their talents to establish the Harvard Lab, where they developed a computer-mapping program called the Synagraphic Mapping System, or SYMAP. This was the first raster-based GIS which employed Dual Incidence Matrix Encoding (later known as Dual Independent Map Encoding, or DIME). Harvard’s SYMAP with DIME was employed by the U.S. Census Bureau in 1967 doing research in New Haven, Connecticut. DIME allowed the development of geographical maps and street addresses for the entire United States by the Census Bureau.

The post-1945 period of unparalleled urban expansion was made possible by the increased mobility afforded by inexpensive personal vehicles and construction of high-speed highways. Engineers began designing these highways with separated grades, which came to typify the burgeoning Interstate Highway System introduced in 1955. While most civil engineers concentrated on developing additional highways and using machinery to carve the Earth to better suit mankind’s needs, urban planners began exploring alternatives to the suburban sprawl they witnessed changing the landscape of the nation’s metropolitan areas. The spokesman for this movement was a

transplanted Scotsman named Ian McHarg, a professor of landscape architecture at the University of Pennsylvania. McHarg described engineers as those individuals “who, by instinct and training, were especially suited to gouge and scar landscape and city without remorse”. These competing philosophies evolved through the 1950s and 60s, giving little portent of the environmental awakening that was brewing. In 1969 Ian McHarg published *Design with Nature*, which argued that form must not simply follow function, but must also respect the natural environment in which it is placed. Up to this time environment had been almost insignificant factor in planning and design because there was no established protocol to quantify and display information about the natural environment. McHarg solved this dilemma by employing a series of transparent overlays, which he felt was the most efficient means to display spatial data so as to convey large volumes of spatial information simultaneously, such that the environmental setting could be adequately appreciated.

McHarg showcased his approach in 1968, when his firm was hired to evaluate the proposed routes for the Richmond Parkway on Staten Island. Highway engineers had recommended a cost-efficient route along a 5-mile stretch of scenic greenbelt parkland, which fomented considerable public opposition. McHarg analyzed the situation with respect to “social values”, which he defined as “benefits and costs to society caused by construction of a multipurpose facility such as a major traffic artery”. His subsequent evaluations included those factors which he judged to be of social value, such as: history, water, forest, wildlife, scenic, recreation, residential, institutional, and land values. He crafted a transparent overlay for each factor, with the darkest gradations representing areas with the greatest perceived values and lighter tones for the least-appreciated values. Then all of the transparencies were then superposed upon one another over the original base map (Figure 1). The result was a “social value composite map”, which was then compared to a map showing geologic and other natural hazard considerations.

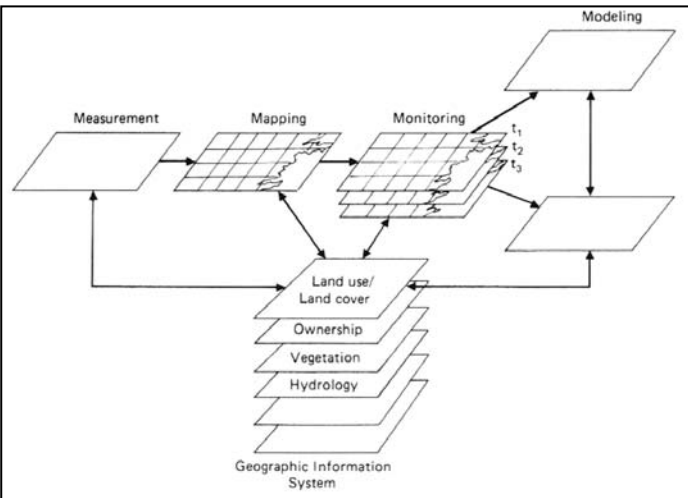


Fig. 1. The four M's of GIS introduced by Ian McHarg: measurement, mapping, monitoring and modeling (from Star & Estes, 1990).

In the end, the highway was moved west of the Greenbelt, saving

the socially valuable forest and parkland. Neither his nor any other proposal was actually built and the Richmond Parkway (now called the Korean War Veterans Parkway) remains unfinished. But, McHarg’s pioneering method heralded the onset of a new era in which composite map overlays have come to dominate the workplace of the engineer, architect and the planner, while influencing decision makers and constituents about all manner of societal issues.

The evolution of GIS from the 1960s to this new 21st century will be described in the following paragraphs. Figure 2 shows the evolution of this technology with respect to the advances in computer technology. GIS’s leap from academia to application came about largely through the efforts of Jack Dangermond, a 1968 landscape architecture graduate of California Polytechnic in Pomona. Dangermond was a grad student at the Harvard Lab in 1968-69 and after his return to California founded the Environmental Systems Research Institute (ESRI). ESRI developed its own in-house system designed for mapping environmental suitability in 1973 when it secured a contract for the Maryland Automatic Geographic Information (MAGI) system, which became a model for most other planning GIS systems. Until 1982 ESRI was a consulting services company. That year ESRI introduced ArcInfo with the help of Scott Morehouse, another former Harvard Lab worker, who they hired as their Chief Software Architect. ESRI and others in the commercial sector have developed and assisted the growth of GIS worldwide, making it the software giant it is today.

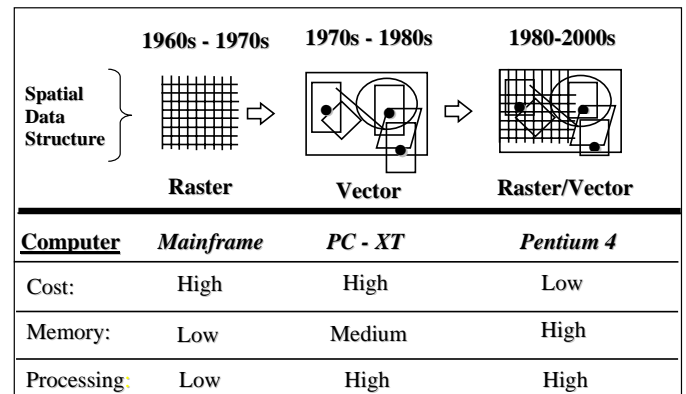


Fig. 2. Evolution of Spatial Data Models and Computers (Luna, 1995).

As more and more electronic resource data was made available through the Landsat program (discussed previously), GIS use increased dramatically between 1972-85. The deployment of the Global Positioning System (GPS) in 1985 provided a rocket boost to an already burgeoning industry. GPS rapidly emerged as the primary data mechanism for navigation, surveying and mapping. The 1980s saw most academic institutions embrace GIS as the primary planning tool, with many using Peter Burrough’s text *Principles of Geographic Information Systems for Land Resources Assessment*, which appeared in 1986. On its heels the *International Journal of Geographical Information Systems* was established, which soon revealed the diversity of emerging research – most being accomplished by British and

American geographers. Also during this time, two centers for research in GIS, the National Center for Geographic Information and Analysis (NCGIA) and the United Kingdom Regional Research Laboratory (UK RRL) were established in the United States and Great Britain, respectively.

While geographers and planners used ArcInfo®, engineering organizations preferred Intergraph®, a company that introduced the first terminal designed to create and display graphic information in 1972. Initially focused on Computer Aided Drafting, Intergraph released the first computer graphics terminal that allowed raster technology in 1980. Appreciating the emerging GIS market, Intergraph spun off a Mapping and Geospatial Solutions division in 1989, which promotes their GeoMedia product line. This has emerged as the primary competitor to ArcInfo for GIS applications.

During the 1990's, GIS began entering into a new phase. In 1992 Michael Goodchild suggested the term Geographical Information Science (GISc) should be applied to what has become its own interdisciplinary science, drawn from the close integration of academic, public, and commercial developers and users of GIS. The information revolution brought on by the Internet has also served as a catalyst for GIS. The Internet has availed enormous data transfers through File Transfer Protocol (FTP) and information sharing through Hyper Text Transfer Protocol (HTTP). These transfer methods allowed GIS users to share data sets and perform research in a shorter amount of time. In 1994 President Clinton signed an executive order creating the National Spatial Data Infrastructure (NSDI) and the Federal Geographic Data Committee (FGDC). The FGDC oversees the NSDI and its goal is to "reduce duplication of effort among agencies, improve quality and reduce costs related to geographic information, to make geographic data more accessible to the public, to increase the benefits of using available data, and to establish key partnerships with states, counties, cities, tribal nations, academia and the private sector to increase data availability".

1994 also witnessed the establishment of the OpenGIS Consortium (OGC) to promote interoperability, or openness in the software industry. Open publication of internal data structures allows GIS users worldwide to build applications that integrate software components from different developers, while allowing vendors to enter the marketplace with competing products that are interchangeable with existing components, just as the concept of interchangeable parts promotes competition in the automobile industry. In the past few years the Open GIS Consortium has emerged as a major force in the trend to openness, as a consortium of GIS vendors, government agencies, and academic institutions.

The development of GIS has been complex and intriguing. GIS has developed into an everyday activity for millions of end users. Through its humble beginnings, GIS has come to the forefront of all the physical sciences and civil engineering over the past four decades and it is here to stay. Although GIS may not meet all the needs of everyone or every situation, it does offer a powerful and

effective tool which is rapidly being accepted by the general populace and decision makers.

COMMON INPUT FOR GIS

Base maps

Maps have played an integral role in the development of the geotechnics; which encompasses soil and rock mechanics, engineering geology, hydrology, hydrogeology and geoenvironmental engineering disciplines. Everything we examine in the physical world is by necessity spatially segregated through the use of georeferencing. The seminal georeference system was latitude (y) and longitude (x) and mean sea level (z). This system provided the requisite controls for planar projection mapping of the Earth and transoceanic navigation until after the Second World War.

As the U.S. Geological Survey began mapping the nation in 1894 most states adopted planar map projection systems that utilized Gauss Kruger principles, which yield increasing distortion with distance from the reference meridian. These rectangular coordinate systems were much easier to use than the complicated latitude/longitude system, so were adopted as State Plane Coordinate Systems (SPCS). If the locations are more than +/- 6 degrees from the reference meridian, their SPCS locations are usually erroneous; but this was not a concern in most of the small eastern states, where the system originated. However, in the vast expanses of the western US, the SPCS have often proven unreliable, which led to many location errors.

After the Second World War the military developed the Universal Transverse Mercator (UTM) system, which allows the curvilinear surface of the Earth to be divided into a series of rectangular boxes with a rectangular system of coordinates, but using longitude as the meridian of tangency instead of the Equator. Distortion increases with longitude as well as with latitude away from the reference meridian. In the upper latitudes the errors increase markedly, but the military didn't contemplate conventional warfare occurring in those regions when they switched to UTM system in the mid-1950s.

The deployment of the Global Positioning System (GPS) in 1985 provided a new low cost alternative for accurately locating positions on the Earth's irregular surface. NOAA turned off selective availability (SA) in May 2000, to stimulate development of the GPS applications in the civil and commercial marketplace. GPS has emerged as the primary data system for all manner of co-location and navigation, down to the individual user on foot. GPS coordinates can easily be recorded electronically and downloaded onto any GIS.

Projection and Registration

Map information in a GIS must be manipulated so that it registers, or fits, with information gathered from other maps. Most existing data is tied to various forms of georeferenced information, such as assessor's parcel maps. Many of these

maps are dated, having been developed before modern cartographic corrections (usually for Earth curvature) were implemented. Older maps must be undergo projection conversion before integrating them into a modern GIS, which utilize GPS georeferencing. A wonderful aspect of most GIS is they incorporate processing subroutines that can transform older data to modern coordinates if a sufficient number of georeferencing points can be co-located on both the old and new maps. These georeference points may be benchmarks, old structures, roads, or even above-ground power lines; anything that can be identified on both maps in the GIS. For normal day-to-day applications, the USGS 1:24,000 scale Digital Raster Graphic (DRG) topographic sheet makes a suitable digitized base map. These are inexpensive and widely available on the Internet. One of the most common examples of georeferencing is overlays of previous shorelines extracted from earlier maps, like that shown in Figure 3.



Fig. 3. Overlay of historic shorelines in Oakland, CA between 1860 and present, overprinted on USGS 1:24,000 scale DRG.

Data Capture

Historically, the most expensive and time consuming component of GIS has been data capture, because prior to 1990, very little geotechnical data was stored in electronic format. This data also often requires editing, as some objects on older maps will need to be specified. Some paper maps can be scanned electronically as raster images, which convert map lines to a series of points and digits. Unfortunately, the blemishes, fading, tears and unintentional marks are also faithfully recorded. Editing of data that has been automatically captured can be burdensome and time consuming. Other data can be input by tracing with a mouse, if there are sufficient reference points that can be input as well, to register location in a form recognizable by the GIS being used. Many GIS were formulated to emphasize spatial relationships between mapped objects, and such boundaries are usually represented by a line. The line may be a road, mapped boundary, or some sort of link between two other points of interest. Civil infrastructure elements, such as roads, may not be reflected accurately, in terms of absolute scale, but simply represented by a default line width(s) coded into the mapping software.

Data Integration

GIS makes it possible to mix or integrate information that would otherwise be difficult to associate through other means. For example, most NRCS soil maps were originally constructed on ortho-rectified aerial photos. These could be scanned, georeferenced and sandwiched with other kinds of data, such as topographic and geologic maps, to prepare hybrid map products. Other forms of data can also be combined into the “mix” to form maps that display trends or predict various responses. For example, in a developed tract of homes using septic systems, water bills could be tied to average monthly usage. By dividing out the irrigable area on each lot, the plat owners who use the greatest volume of water could be identified and areas of heavy septic discharge could be estimated spatially on the hybrid map.

Data Structures

Digital geospatial data is collected and stored in many different formats. A GIS must be used to convert data from one type of structure to another, without corrupting the data. Satellite data can usually be “read” into the GIS in a raster format. Raster data files consist of rows of uniform cells coded according to data values. Raster files can be manipulated quickly by computer, but they are often less detailed and may be less visually appealing than vector data files. Vector digital data files have been captured as points, lines (a series of point coordinates) or areas (shapes bounded by lines). A typical vector file would be tax assessor’s parcel maps. The evolution of vector/raster data structures is also shown in Figure 2.

Data restructuring is a crucial aspect of GIS if engineering and traditional cartographic data are to be combined into similar formats, so they can be evaluated concurrently. GIS routines are available that can convert a satellite image to a vector structure by automatically generating lines around electronically visible “cells” with the same classification, while determining the cell spatial relationships. Engineering information, such as infrastructure improvements, is almost always in a vector format, while topographic maps are almost always in a raster format. Vector data looks more crisp when outlining man-made improvements or linear boundaries, but raster data looks better for naturally occurring features, such as streams or forest clearings, which have irregular or curvilinear outlines.

Data Modeling

GIS allows two and three-dimensional characteristics of the Earth’s surface, subsurface or atmosphere from geospatial data. Most data contouring is accomplished using subroutines that utilize either linear interpolation or the mathematical principles of Kriging. Kriging generally yields much smoother curves than the interpolation method. Some common examples of data modeling would be creating isohyets from rainfall station data or contouring groundwater levels. These data models can then be combined with other types of information layers in the GIS. Some common examples would be: combining measured rainfall isohyets with elevation, or the thickness of a certain geologic

formation (isopach) as compared to the depth to its upper surface (isopleth).

Another form of data modeling is commonly termed “feature extraction”. Here the GIS is programmed to recognize both the spectral and physical signature of specific types of features, such as pavement or structures. The GIS can “view” the raster data, synthesize it, identify specific features, then draw the areal limits of these features. It can also calculate a wide range of physical attributes, such as the aggregate area within these bounds.

Data modeling has often proven useful in ferreting out key factors that influence a physical attribute within a given data set.

Unfortunately, dynamic factors, such as seasonal or annual changes in such physical features are not always available for inclusion in the dataset, and such factors can, therefore, be easily overlooked.

COMMON ANALYTICAL METHODS USING GIS

Information “Layers”

The manner in which geospatial data is stored or filed as “information layers” in a GIS makes it possible to perform a multitude of complex analyses. Not all of these analyses need be “real”. For instance, a governing body can spell out which physical attributes they wish to see included in a hybrid analysis and these factors can arbitrarily be “graded”, on any rating scale that is chosen. For instance, a city planning commission may decide that they want to create a “development capabilities map” of their jurisdiction based on: 1) underlying soils; 2) mapped landslides; 3) ridgeline exposure; 4) woody vegetation density and, possibly, 5) expansive soils potential. These factors can be weighed equally (e.g. 20% each, if five factors) or weighed with decreasing importance, however the commission sees fit. Weighting factors are usually influenced by public input and sentiment. The resulting map would not be anything “real”, but an artificial product of the input data being weighted, combined and compared by the governing formulae. These sorts of planning documents are becoming commonplace across the country.

Information retrieval

As geotechnical engineers, we are often asked “What do you know about this site?” GIS systems allow us to pour through large volumes of map information and select whatever information is reported on any given location. In most instances, scanned aerial photographs (DOQQs) or DRGs will provide a useable base for other kinds of geospatial information. Another common map “layer” is the assessor’s parcel boundaries. These must be georeferenced to ascertain where the subject parcels are located with respect to the physical ground or water surfaces. Environmental restrictions or sensitivities may be modeled as well by the GIS if development guidelines such as creek bank or ridgeline setbacks, designated wetlands or green space limits are clearly defined.

Topological modeling

A GIS is very effective at recognizing and analyzing spatial relationships between mapped features, such as old wells, highways, structures, or potential pollutant sources, like storage tanks. Topological modeling allows easy determinations of distance or proximity from such features, telling us how close a certain data point is to our specified location. In some cases these distances are crucial to site development decisions, such as offsets from water wells and septic tanks/leach fields. Recognized hazardous or toxic waste sites are listed in a nationwide data base maintained by the USEPA and this data is easily downloaded and converted to most GIS.

Networks

Networks are commonly used in contingency planning and forensic assessments. We can lay out any scenario, such as an accidental leak, and have the GIS calculate how long it would take for a particular spill or pollutant to travel certain distances. A GIS can simulate the travel path of any viscous material along a prescribed path, which can be backed out of stand-alone flow estimates from established software routines, such as HEC-RAS. This sort of analysis is useful for developing containment plans for accidental leaks, flooding, or routing of debris flows.

Overlays

Overlays are commonly employed by planners to group multiple physical, biological or aesthetic aspects into hybrid map products that exhibit the relative sensitivity of the interplay between the chosen factors. Some of the most common factors are intermittent wetlands, perennial water courses, soil type, erosion potential and ground cover. Geologic hazards may or may not be recognized, or quantifiable for rational input. In some cases, entire formations are entered and negatively weighted because of past experience with that particular unit or soil type. Though not scientific, such lumping is a common practice, based on some imagined or assumed risk.

Data output

Another critical component of GIS is its ability to produce pleasing graphics that convey analyses to decision makers and the public at-large. These analyses usually begin with entering any codified restrictions, such as structural setbacks. The included attributes can then be electronically combined and weighted according to arbitrary values set by the body ordering the analysis. Such hybrid “maps” frustrate many engineers because they can arbitrarily be weighted to restrict or even eliminate development from areas where the project’s detractors reside on adjacent parcels with all the same attributes! Planners accept the premise that limiting future development tends to create a more pleasing and aesthetic environment for the residents that are already established somewhere. Because of this view, planners are more swayed by simple spatial comparisons than by other physical factors, such as traffic safety, fire safety (water storage), emergency vehicle access and other engineering-related features that tend to encroach the green belt.

GIS has rapidly emerged as the preeminent mechanism by which potential environmental impacts are evaluated. Existing data of any watershed can be modeled to show the progressive physical effects of proposed residential, commercial or mining schemes. Models of physical processes, such as runoff and erosion, can then be run on the hypothetical development to test what the expected environmental impacts might be.

CHALLENGES WITH THE GIS REPRESENTATION OF GEOTECHNICAL DATA

Resolution versus scale

One of the early problems with GIS for engineers was the small scale representations because low resolution digital information was often used in the analyses, usually from Landsat. The early data sets often had resolutions of 100 to 200 m, which made them poor predictors of site-specific information. They were useful for regional and geologic/soil surveys and for post-disaster assessment. Over the past decade the most common resolution has dropped to 30 m, with 10 m increasingly common. 1 m and 2 m digital data is rapidly coming online for site-specific inventories and investigations. 2 m and better resolution allows structural details such as buildings and pavement to be readily identified and is useful to engineers making site-specific investigations. In summary, small scale maps provide little resolution and are used for interpretation of large areas, typical for geological studies. On the other hand, large scale maps provide more site-specific detail and are used for interpretation of smaller areas, typical for engineering studies. The issues of resolution and scale are converging with modern technology and will soon be less of an issue as image resolution and the ability to process data keeps advancing.

Handling the 3D component represented in maps

Unlike planners, geopracticioners work with data derived from beneath the Earth's physical surface, requiring attention to the "z axis". Most GIS were not set up to store, synthesize or analyze subsurface geologic or hydrologic information.

Fortunately, a great number of software programs have been marketed to store subsurface data in an electronic format suitable for manipulation on most commonly-employed GIS (ESRI, Intergraph, MapInfo, EVS, etc.). These subsurface data management programs include: gINT, ISIS, TechBase, ViewLog, StratiFact, EVS-CTech, ArcIMS, OpenWorks, GeoMedia, EQuIS, LogPlot, Borehole Mapper, LD4, pLog, Modflow, dBase and Paradox. Most data can be linked to commonly-employed GIS to enable graphic displays and commingling with other kinds of geospatial data.

In spite of all these program aids, disparities in subsurface information between adjacent borings will continue to cause problems in interpretation and frustrate end users. When subsurface data between adjacent borings is contrasting, some evaluation and interpretation utilizing professional judgment will

have to be made. Common problems include: data varying according to what individual was logging the holes; the nomenclature used by different individuals; nomenclature changes and shifts in interpretation that have occurred over time; and physical separations caused by an array of natural causes, such as faulting, lithologic contacts, erosional truncation or facies changes.

These interpretive variances will remain at-large for the foreseeable future because geopracticioners commonly gather subsurface data from a variety of sources, including published geologic maps which can exhibit contrasting interpretations and unit nomenclature on adjacent quadrangles.

Disparities in age and quality of subsurface information

A major problem for geotechnical data is the disparity and age of much of the collected data. Historically, there have existed wide variations in drilling methods, sampling intervals and the geologic interpretations derived therein. For instance, a "bedrock" contact may be interpreted whenever a drive sampler encounters a clast larger than the sampler. The reliability of the recorded subsurface geologic data is always subject to the experience of the interpreter. With the passage of time there have been repeated historic changes in stratigraphic nomenclature and geologic age dating. Environmental changes, such as ground water chemistry have also been documented in most areas that draft large volumes of groundwater and undertake recharge. There also exists inherent variability in the disposition of the weathered bedrock profile, which is often subject to interpretation because the geophysical properties may not reflect gradual changes, only pronounced shifts. Old wells may also be mis-located because they were drilled well in advance of developed improvements, such as streets.

Well log nomenclature and annotations

Well logs were normally annotated as a function of the well's intended purpose. In water wells piercing shallow aquifers, there is often scant detail available on the logs filed with most state agencies. But, the depth of the well often tells a story of itself, because well drillers seldom bore beyond the economic limit for extracting water. Explaining an anomalously deep well can sometimes prove valuable to understanding the subsurface hydrology (sometimes the drillers went deeper to pierce fresh water, well beneath brackish water that infiltrates most coastal aquifers).

Geotechnical borings commonly contain abundant descriptive detail, but are usually rather shallow. In most instances the record of sample recovery contains as more valuable information than the descriptive log of the boring itself. Subaqueous geotechnical borings generally exhibit highly variable recovery, depending on the rig and experience of the drillers and may not be as predictive of actual conditions.

Wells drilled by the petroleum industry are usually very deep and are accompanied by excellent geophysical logging, commonly employing electrical potential, resistivity and gamma ray logs.

These can paint a detailed picture of the subsurface stratigraphy and groundwater chemistry. However, the evaluation of e-logs requires specialized expertise and experience with interpretation. Rotary wash borings undertaken for deep water wells and petroleum extraction also employ standardized recovery corrections for well cuttings, which are a function of depth, rotation of the drill stem, drilling mud viscosity and cuttings circulation.

The lithologic contacts logged by most geologists or drillers may not coincide with the geophysical properties boundaries, which are of interest to the geotechnical modeler. Residual weathering profiles are characterized by high variability and some types of weathered bedrock exhibit physical properties similar to the overlying residuum. Hammer or penetration tests provide a comparison in behavior are valuable to the engineer trying to characterize a site.

Two-dimensional representations

One of the most difficult aspects of GIS representations of geotechnical data is the two-dimensional representation of three-dimensional situations. The depths and thicknesses of map units can be represented with isopleths; or lines of equal depth or elevation. Isopachs represent lines of equal unit thickness. Both of these representations are akin to topographic contouring of subsurface geologic structure and stratigraphy. Such contours are typically overlain on a geographic base.

The depths of geologic units mapped on the earth's surface may be unknown. End users can draw incorrect conclusions from such representations because most geologic units are spatially discontinuous and their grain size distribution varies laterally and along their former axis of flow/deposition. Some examples of geologic units that commonly exhibit asymmetry are: landslides, buried debris fans, liquefied materials, alluvial materials, channel deposits, aeolian deposits and estuarine units.

Geotechnical data assumed to be of like quality

The geotechnical "data" presented to end users of GIS products is commonly an "information layer" that is visually construed to be of equal quality and reliability, regardless of its source. This is because data points relating similar TYPE of information appear similar, without any hint of their reliability. As a culture, we have been conditioned to assume all data points on a given map have been verified by some governing third party. But, in areas where there is scant data, even poor data is seen as being better than no data, so it is usually included.

The variance in source information for GIS work products sets up inherent limitations, similar to those which exist in computational analyses. An appreciation of the historical evolution of engineering geology, geotechnical engineering, petroleum engineering, seismology and water well exploitation methods are key to formulating opinions drawn simply from such "collected data".

EMERGING SENSORS AND SYSTEMS THAT WILL IMPACT GIS

Digital aerial imagery

Digital aerial photographic systems are rapidly emerging as a cost-effective means to perform surveys of project areas. Although the unit cost is higher for areas up to about 1 square mile, it becomes more cost effective when surveying large tracts of land. Most digital aerial survey systems are comprised of four basic components: 1) a digital sensor (camera and lens); 2) an Inertial Position and Orientation System attached to a GPS to record location and altitude information; 3) an on-board computer to store the collected data; and 4) some sort of flight management system to insure the correct paths and altitude are flown by the sensing platform (aircraft). Most systems are designed to achieve 1 m spatial accuracy from 10,000 feet above the sensed surface. On most flights the achievable resolution is about 0.3 m. By flying at lower altitudes some vendors have demonstrated imagery with 0.22 m resolution and 0.50 m horizontal accuracy over extremely rugged terrain (Liszewski, 2003). Visible light spectrum (color) or color infrared are normally employed as recordation media. Color depth is far greater for digital imagery than for film. This translates to a greater density of discernable information on the digital image. Digital media is also more stable and is ready to use; almost as soon as the aircraft lands. Digital imagery has the added bonus of flying below clouds, along prescribed paths and at different times of the year. The output is already digitized and georeferenced, and is easily input into a GIS and orthorectified.

LIDAR

LIDAR is an abbreviation for Light Detection And Ranging. It is a scanning methodology which uses high powered laser and laser receivers, a sensor-mounted inertial measurement unit, a sensor-mounted GPS receiver and a ground-based GPS station. LIDAR has shown great promise for terrain resolution. LIDAR surveys are usually imaged from altitudes between 3,000 and 6,500 feet above the subject terrain with a Nominal Ground Sampling Distance (GSD) of 1.5 m (dual pass) to 5 m (single pass) and a Root Mean-Square Error (RMSE) of between 0.2 and 2 meters horizontal and 0.12 to 0.2 m vertical. It provides excellent first return reflections of vegetation canopy and structures and an intermediate return from mid-story vegetation. The last return is close to the actual ground surface, so the "bare-earth surface" can usually be determined from last-return data processed to remove data points which did not penetrate vegetation or structures.

Accuracy claims for LIDAR-derived elevation products are based on comparison to test points located in open terrain (i.e., where the sensor has an unobstructed view of the ground surface.) However, LIDAR elevation surfaces are frequently produced over areas of tall or dense vegetation, for which, little knowledge of achievable LIDAR accuracy exists. These problems are the focus of much research and validation at the present. LIDAR can give excellent results compared to aerial photography, especially in regards to sensing the ground surface

beneath tree canopies, revealing the actual character of the underlying ground surface (Haugerud, et al, 2003).

INSAR

INSAR stands for Interferometric Synthetic Aperture Radar. It was recently developed as a remote sensing technique using radar satellite images from ERS1, ERS2, JERS, IRS or Radarsat.

These satellites shoot constant beams of radar waves towards the earth and record them after they bounce back off the Earth's surface. Two data sets compose the images, which are often referred to as interferograms. One set records how much of the wave reflected back to the satellite (signal intensity). This depends on how much of the wave has been absorbed along its travel path and how much has been reflected in the direction of the satellite. The second data set is the 'phase' of the wave, which depends on the distance and shape of the ground object from which it reflected.

Every pixel in radar satellite image is comprised of these two data sets: the intensity and the phase. The intensity can be used to characterize the material in which the surface the wave bounced off is made of and what orientation it has. Oil leaks on the sea, for instance, can be spotted in that way. They look much smoother than the surrounding water.

The phase is used in another way. When the radar satellite revisits the exact same portion of the Earth, the phase image should be identical. If it is not the case, then something has been going on. And by combining those two images, scientists can measure how much and where the ground surface has moved.

Though expensive, the strength of INSAR lies in its ability to provide observations of change in ground position. Ground fissures, settlement, or dilation are all easily discerned with a high degree of spatial accuracy. Movements of only a few millimeters in images with 20 meter spatial resolution covering 100 km spatial extents are obtainable. INSAR has a remarkable ability to detect emerging ground fissures and accurately track the growth of such features on repeated passes.

Multispectral Imagery

Multispectral imagery is digital information collected across a broad range of the electromagnetic spectrum in both the visible and nonvisible light ranges, using a multispectral scanner. These scanners can sense on as many as 300 channels, gathering terabytes of information in a single pass. Multispectral analysis considers all the bands of a particular image as part of a single package or unit of information. Multispectral imagery is collected to be used together rather than as individual images. For example, the seven bands of NASA's Landsat Thematic Mapper could be displayed as 210 different composites. A Multispectral Imagery Interpretability Rating Scale (MIS-IIRS) protocol has been developed which characterizes multispectral imagery as a package of data (multiple bands) with a single inherent interpretability.

Selecting the spectral bands that best discriminate the materials or features of interest is generally of the utmost importance. There are few rules for this selection, as every case is viewed as being somewhat unique. The choice of bands depends on the features to be discriminated and their immediate surroundings. This selection will vary by feature, locality, season, time of day, and task. It is left to the exploitation expert (interpreter), on a case-by-case basis to determine which composite best assists feature discrimination.

Once the preferred bands for maximizing spectral contrast have been selected, the color display presentation does not significantly influence interpretability. If a feature/background contrast exists, it will be apparent in all presentations using those bands even though there may be a subjective preference for one presentation over another. For example, while the colors differ in all six permutations of the three-band composite figure, large buildings can be spectrally distinguished from trees, standing water, or relatively fresh concrete in any image. However, aged concrete does not radiate spectrally much different from dried grass on many bands.

Hyperspectral Imaging

Great progress has been made in the use of remotely sensed data. In the early 1970s, NASA initiated the LANDSAT program, which provided images useful for evaluating the earth's resources. In the late 1970s and 1980s, sensors with increasing spatial and spectral resolution were developed. This greatly extended the usefulness of remotely captured images. The hyperspectral remote sensors developed in the late 1980s and 1990s raised the use of remotely sensed data to a new level.

The key characteristic of hyperspectral imagery data is the high spectral resolution that is provided over a large and continuous wavelength region. Each pixel in a hyperspectral image is associated with hundreds of data points that represent the spectral signature of the materials within the spatial area of the pixel. The result is a three-dimensional data set (or "image cube", see Figure 4) that has two axes of spatial information and one axis of spectral information. This is in contrast to multispectral imagery data, whose pixels are associated with a few (7 to 15 bands) low spectral resolution images taken over a large but non-contiguous wavelength region. The high resolution of hyperspectral imagery makes it possible to uniquely identify different materials at the earth's surface as opposed to being limited to discriminating between the broad spectral classes, which can be derived from multispectral imagery.

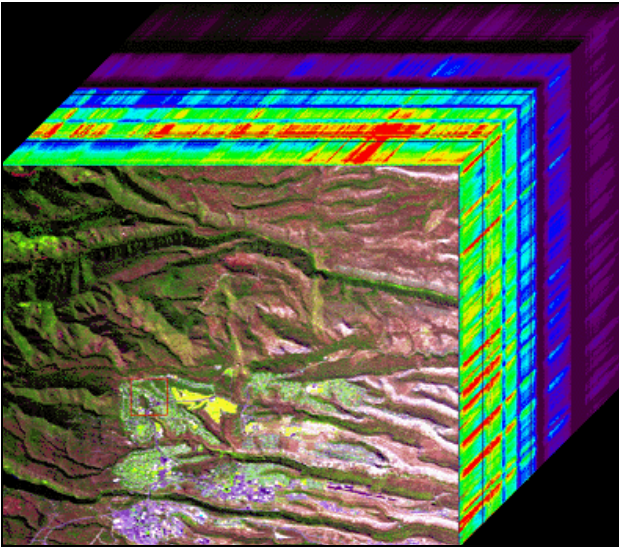


Fig. 4. Hyperspectral Image Cube (adopted from NASA)

Hyperspectral imaging technology is being used increasingly in environmental monitoring, geologic characterization, transportation, precision agriculture, and forestry applications. However, this technology has yet to establish a foothold in geotechnical engineering. The traditional methods of site characterization such as drilling, penetration, and geophysical techniques still prevail in geotechnical engineering practice. These technologies are increasingly being geo-referenced for use, analysis, and management in information systems, and the interpretation of subsurface conditions still requires engineering judgment and experience. The challenge with borehole data is that the subsurface data collected is only valid for a small representative area/volume around the discrete sample/measurement and there is often a need to interpolate between data. Uncertainty increases away from the measurement locations. Therefore, there is a need to promote the use of information technologies to enhance the traditional methods in geotechnical engineering practice. Hyperspectral imagery captures the spatial information as well as the spectral features of the earth's surface. It provides abundant data for the surface classification and characterization of geomaterials on a pixel-by-pixel basis. Although it only studies surface conditions, this technology can still give us valuable information for the geotechnical practice.

One of the main applications of the hyperspectral imaging technology in geo-engineering is mineral identification, because mineralogy is a key factor to determine soil and rock characteristics. Research done in this area has found that different minerals have different spectral signatures. The spectral signatures of minerals were used by researchers in Colorado to map expansive clays in the field. Hyperspectral data was also used to study the soil/rock properties in a borrow site.

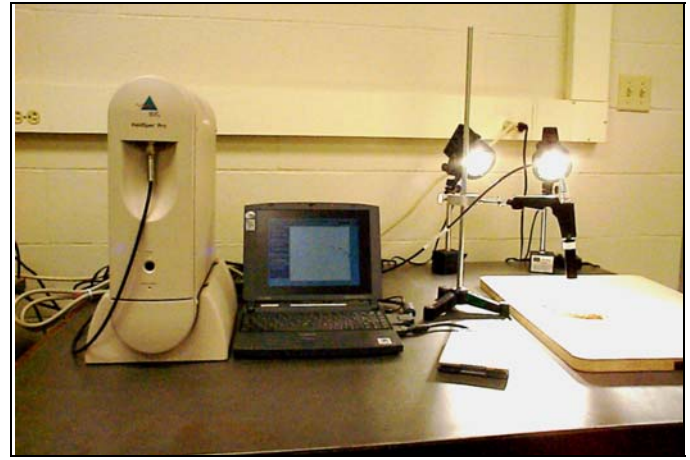


Fig. 5. Spectral Laboratory Setup at UMR

Ongoing research at the University of Missouri - Rolla is exploring the fundamental relationships between the spectral signatures and the properties of soils. A FieldSpec Pro spectroradiometer, manufactured by Analytical Spectral Devices, Inc., has been used to capture the reflectance spectra of soils in a wavelength range from 350 nm to 2500 nm (Figure 5). The important factors that influence the soil spectral properties have been identified, and how they affect the soil reflectance is being studied. Water content in a soil was determined based on the spectral data and the use of neural network algorithms. To better understand the spectral response of soil mixtures with different compositions (end-members), several well-characterized clay minerals were mixed with known quantities to make different mixtures. These mixtures were then measured spectrally. The un-mixing algorithms were applied to the mixture spectra to determine the abundance of the end-members. The results show that the abundance of the components in a mixed soil can be obtained based on the spectral measurements. To use remotely sensed data in geotechnical engineering, spectral un-mixing has to be applied because each pixel is associated with a soil mixture. By doing spectral un-mixing, different maps can be developed (e.g., water content distribution and expansive clay distribution maps). These maps can be input into a GIS system, which can be used to solve various geotechnical problems along with other information.

**CASE STUDIES IN GEOTECHNICAL ENGINEERING
CASE STUDY 1:**

Real-Time Monitoring of Incipient Rock Slope Failure

On March 22, 1998 a composite earthflow landslide involving 17 million m³ of weathered rock and ancient slide debris began moving down from Mission Ridge into a residential areas lying 1.67 km below in Fremont, CA. The maximum depth of sliding was about 35 m and the headscarp reached an average height of about 20 m. Within a few days large tension cracks developed in the unfailed sandstone, up to 100 m above the receding headscarp (Rogers and Drumm, 1999).

The series of coalescing earthflows moved about 150 m downslope, threatening some homes. The movement slowed to an imperceptible crawl within just a few days. Two months later the exposed headscarp began retreating, dumping approximately 46,000 m³ of new material onto the head of the recently-active landslide (Jurashius, 2002). The block that was moving involved about 185,000 m³ of previously unfailed material, a brittle sandstone and shell-rich coquina (Jurashius, 2002).

A pair of invar extensometers were installed across a prominent tension crack soon after it appeared, in late March 1998. This was tethered to a telemetry network using a cell phone in late April 1998. This array recorded 0.71 m of movement between late March 1998 and January 2000, with the average rate of creep dropping to just 2.5 mm/month during 1999 (which was unseasonably dry). The block seemed to creep in proportion to precipitation, mostly during the wet winter months (Geolith, 2000). In January 2000 the extensometer array was replaced by GPS receivers installed by the U.S. Geological Survey, shown in Figures 6 and 7.



Fig. 6. Looking upslope at the eroding headscarp of the 1998 Mission Peak Landslide in Fremont, CA (from LaHusen and Reid, 2000).

Figure 6 shows the massive sandstone block with prominent tension cracks. The complete GPS master station (MS) is on stable ground near the ridgetop. The remote instrument station (RS) was located downslope but just off the block for survivability. The remote GPS antenna (RA) was placed on the block and cabled to the remote station.



Fig. 7. The lower station was located on the moving block. Both GPS and radio antennas are on the mast near the electronics package inside a box with a 20 watt solar panel.

The massive block reactivated in late February 2000, initially moving at less than 1 cm/week, then accelerating to twice that velocity, in apparent response to increased rainfall (Figure 8). The block decelerated at the cessation of seasonal rains at the end of March 2000, but remained moving at a rate of 1 mm/week until late July. About 5 cm of cumulative displacement were detected over the 4 month period from February 1, 2000 to June 1, 2000 (Figure 9).

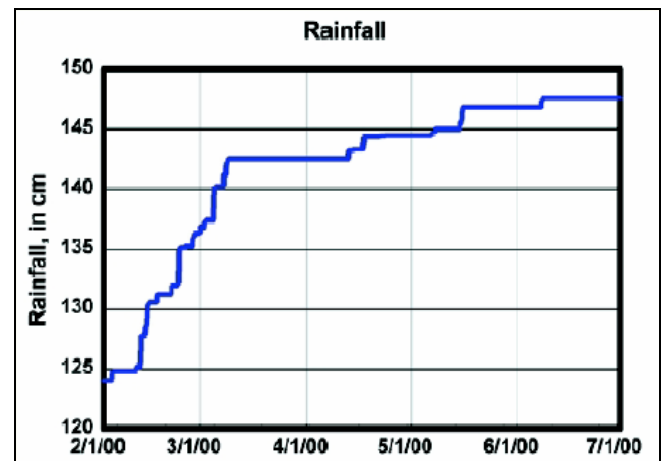


Fig. 8. Rainfall recorded between Feb-July 2000 on the ridge adjacent to the GPS receivers (from LaHusen and Reid, 2000)

The inherent noise in GPS measurements can be seen in Figures 10 and 11, showing all of the individual fixed static solutions. These typically showed repeatability +/- 1 cm horizontally and +/- 2 cm vertically. In order to better discern and visualize trends in the time-series, the median values for of a variable number of individual static solutions were determined (Figure 11). This simple approach was found to be very effective in removing noise from the data and discriminating subtle movements.

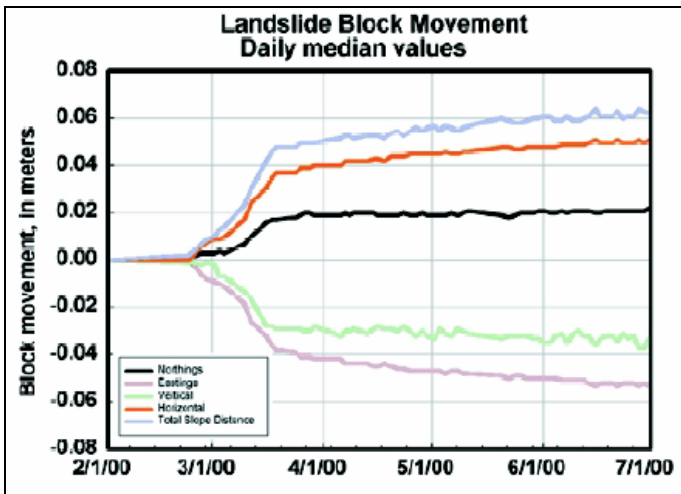


Fig. 9. Recorded median values for horizontal and vertical motion of the incipient landslide block between February and July 2000 (from LaHusen and Reid, 2000).

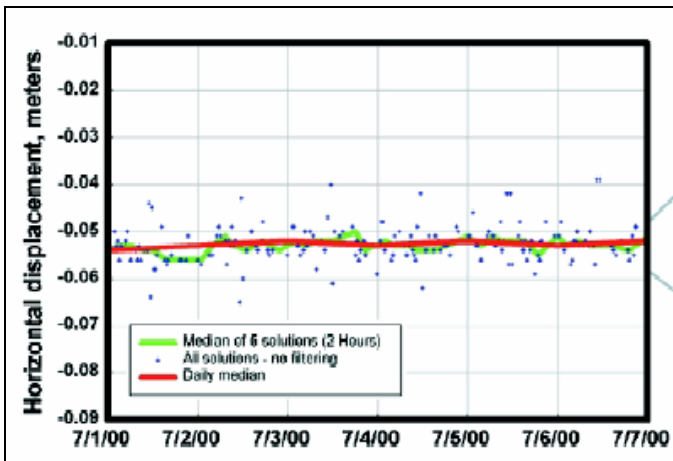


Fig. 10. Daily median horizontal movement shown by thick solid line. Note noise in recorded movements, which is typical.

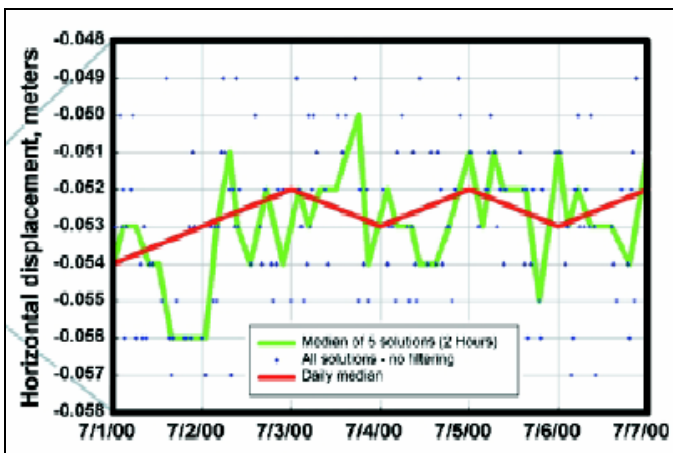


Fig. 11. Detail of GPS measurement noise, as recorded, median of five solutions (see saw line) and daily median (slight see saw). Data taken from LaHusen and Reid, 2000.

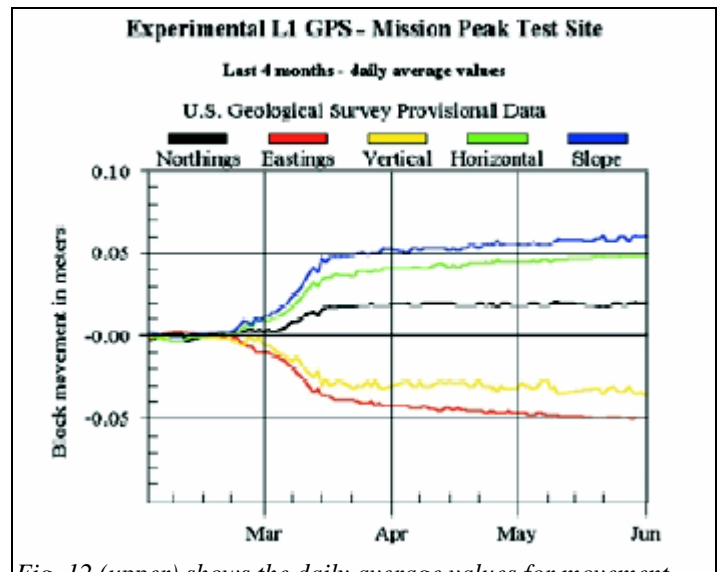


Fig. 12 (upper) shows the daily average values for movement from March to June 2000, as posted on the USGS website.

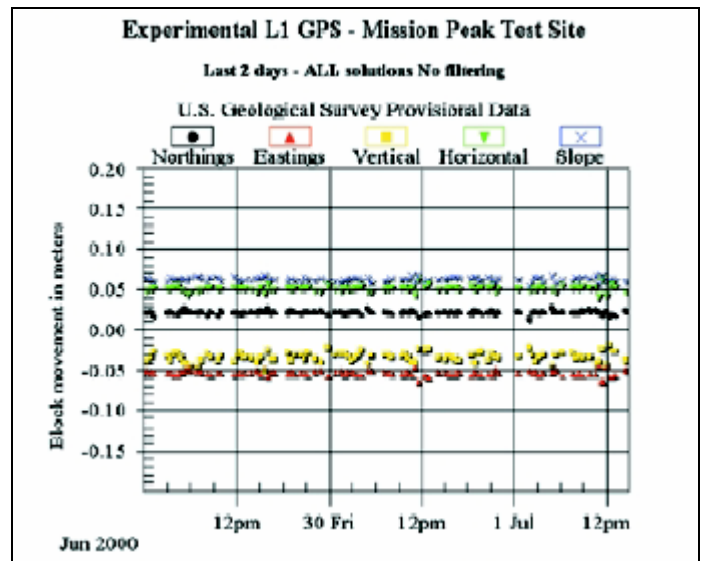


Fig. 12 (lower) shows a typical plot of unfiltered displacement data for a two-day period, in June 2000 (from LaHusen and Reid, 2000).

Near real-time data was displayed on the Internet for City engineers and the general public, so they could judge the state-of-activity of the block. The area is close to the public, but adjoining open space is heavily traveled as recreational open space. Figure 12 present graphs of filtered and unfiltered solutions that were automatically updated every thirty minutes and served via phone or network connections for posting on the Internet.

The automated GPS system provided near real-time monitoring of a remote rockslide hazard and made this available to the general public, with 30 minute updates (LaHusen and Reid,

2000). The modular design used a low-power controller (USGS V2000) to store and forward raw data from a variety of GPS receivers to a Windows-based PC that controls the remote stations and intermittently calculated fixed static solutions. Initial short baseline (<10 Km) applications were configured using L1-only Marconi Allstar receivers and Waypoint Precise DLL for processing (Figure 13).

Individual solutions were obtained twice per hour from 5-20 minutes of 10-second data showed repeatability of 1 cm horizontal and 2 cm vertical. Simple filtering by finding median of 5 (2 hours) and 48 (24 hour) solutions allowed clear discrimination of sub-centimeter movements.

The monitoring scheme was very simple, being comprised of two basic units: a field station and a base station, as shown in Figure 13. The baseline length was 70 m. GPS measurements were stored, forwarded and processed for 20 minute segments of 10 second interval L1 data and the website depiction was updated every 30 minutes.

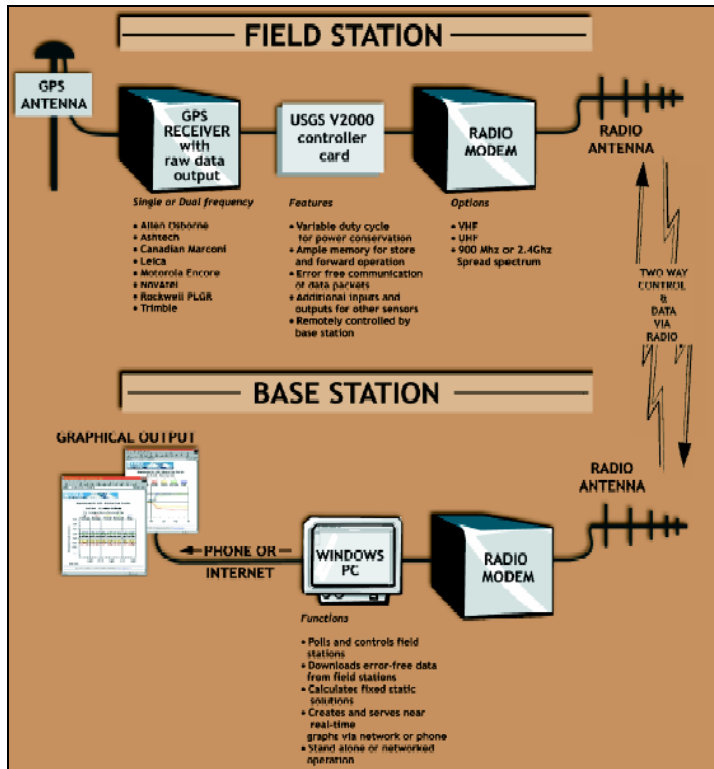


Fig. 13. Monitoring scheme employed at Case History 1 (from LaHusen and Reid, 2000).

This was a pilot study intended to demonstrate how rigorous geotechnical data collection could be applied to provide near real-time monitoring of an impending slope failure using off-the-shelf GPS receivers. The interpretation of the slope stability problem was only based on three reference points. In the past few years our ability to simultaneously record data at multiple points has improved dramatically, and simultaneous monitoring of dozens of benchmarks has become relatively commonplace. With this increasing volume of data collection, a new need is

emerging for interpreting such data spatially with the aid of GIS so relative motions can be tracked. Some of these studies are showing compelling evidence of cause-and-effects between adjoining blocks. A major goal of real-time monitoring is to enable discernment between relatively low risk slope creep from higher-risk accelerating motion, which usually precedes catastrophic detachment. When combined with imagery, movement data and other data layers can be combined to enhance the geotechnical interpretation and allow us to advise clients with some reasonable measure of reliability. The following case histories present some of these more recent advances.

CASE STUDY 2:

Treasure Island – 400 Acres of Geotechnical Data

Treasure Island was built in the late 1930's using a containment rock dike and hydraulic filling. The source for most of the fill came from the bottom of the San Francisco Bay and consisted of sands and mixtures of sand and silts. The Navy has been interested on the overall seismic stability of this site and in the early 1990's subsurface investigation programs were conducted to complement the existing geotechnical data for the island. Since most of the shallow soils are susceptible to liquefaction (e.g., saturated sands), the question of the extent of liquefaction became of interest resulting on a need for spatial liquefaction evaluation. This objective required data from a combination of sources including the Fire Station NGES site. Most of the spatial geotechnical database was populated with data obtained from the NAVFAC Western Engineering Command. The geotechnical data was obtained by a series of San Francisco Bay Area geotechnical consultants subcontracted by the Navy since the early 1940s. This resulted in varying levels of quality in the data and motivated the development of a systematic method to assess borehole quality. This methodology can be used by other organizations, like the US Navy, Cities, and DOTs that need to manage large amounts of geotechnical data.

The first order consequences of earthquake hazard analyses are appropriate for regional and preliminary assessment of the hazard, while second order consequences are intended for site specific and design phase evaluations. For example, liquefaction of a relatively thick stratum at depth may have minimal effect on the performance of an over-lying structure, however liquefaction of a near surface thin layer of soil may have catastrophic implications on the performance of the same structure. Two-dimensional liquefaction hazard maps are generally unable to distinguish between these two occurrences of liquefaction and thus may lead to incorrect and conservative estimates of liquefaction potential. On the other hand, if the analyses focus on second order consequences, such as deformations, a more realistic estimate of earthquake induced damage can be developed. For example, after evaluating the liquefaction potential of each layer in a given stratigraphy the vertical liquefaction-induced deformation for each layer can be computed. Then the total vertical deformation is estimated as the sum of the individual layer deformations and presented as a map or plan showing contours of total vertical settlement.

The advantages of evaluating a geotechnical hazard in a spatial environment have been outlined in a number of publications in the recent literature (Miles and Ho, 1999; Kiremidjian, 1997; Luna, 1995; TC4, 1993). The level of detail of an analysis depends on the scale of the study. For example, a regional study may not use detailed borehole data while, a reasonable amount of geotechnical subsurface data (SPT and CPT soundings) distributed throughout the site may be available for project scale studies. Design level liquefaction evaluations are performed at the site-specific level (harbor site, nuclear plant, dam site, etc.) and involve detailed analysis. The spatial distribution of settlements can be used to determine the differential settlement. This paper describes the progressive development of a system that used Treasure Island data to integrate a desktop engineering GIS with software routines to compute the spatial distribution of liquefaction potential index and deformations resulting from earthquake induced liquefaction. The advantages of performing such analyses within a spatial framework compared to using more conventional non-spatial approaches are illustrated.

Brief History and Sources of Data

Treasure Island was originally conceived as a mid-bay airport, but the plan was soon modified to provide a site to celebrate the completion of the Golden Gate and San Francisco/Oakland Bay Bridges. These events took the form of the 1939 Golden Gate International Exposition. In 1941, the Navy took control of the island as a Naval Station for the war effort. Since then, the U.S. Navy has retained jurisdiction of the island. The island dimensions, 1672 meters long by 1035 meters wide (397 acres), were dictated by the requirements for the airport planned to replace the exposition after closure. The island is relatively flat with an interior ground surface varying from approximately elevation 2 to 4.4 meters Mean Low Low Water (MLLW). The top of the perimeter dikes varies in elevation from 3.2 to 4.9 meters MLLW (Geomatrix, 1990). In the mid 1990s, this Naval Station was in the process of being decommissioned to become part of the city of San Francisco. The US Navy via the Treasure Island Site Manager for NGES, Richard Faris, provided access to

the historical geotechnical data. Additionally, dynamic soil properties reported by Pass (1991) and other investigators at the site were also very valuable for the studies reported herein. The NGES data for Treasure Island was obtained in 1995 in a floppy disk format and most of the field data consisted of CPT sounding. Currently, most of the data is available on their official Internet website: <http://www.unh.edu/nges/>

Historically the most common means of recording subsurface is by the use of the borehole log or boring log. This document contains data from field and laboratory tests making the information a compilation of measured and interpreted data. Usually the document contains some form of header information that pertains to the general borehole and the depth information that contains sampling, testing results and drilling notes. Evaluating the quality of subsurface data may be a very subjective process and will vary based on the purpose of the evaluation. One of the advantages of creating a database for use in a spatial environment (i.e., GIS) is the ability to combine multiple sources of borehole log information. The process of creating a database requires initial data collection efforts for the area of interest. However, a subsurface investigation is typically performed by a consultant/investigator for a specific purpose, and due to budget constraints, only data pertinent to the intended purpose is collected. For example, a borehole advanced as part of a study to determine the shear strength of a soil will use different sampling and testing techniques than a borehole that is drilled to determine the contamination level of the soil profile.

It is well known that the equipment and test methods used to obtain a standard penetration test N-value have an effect on liquefaction analysis. The common procedure to evaluate liquefaction potential in practice can be summarized in the following simple steps: (a) perform boring and sampling using SPT, (b) synthesize results of the field testing (when available) and correct data as appropriate, and (c) calculate the factor of safety for liquefaction using the corrected field data. There are components within each of these steps that may have a significant impact on the computed liquefaction potential (in the

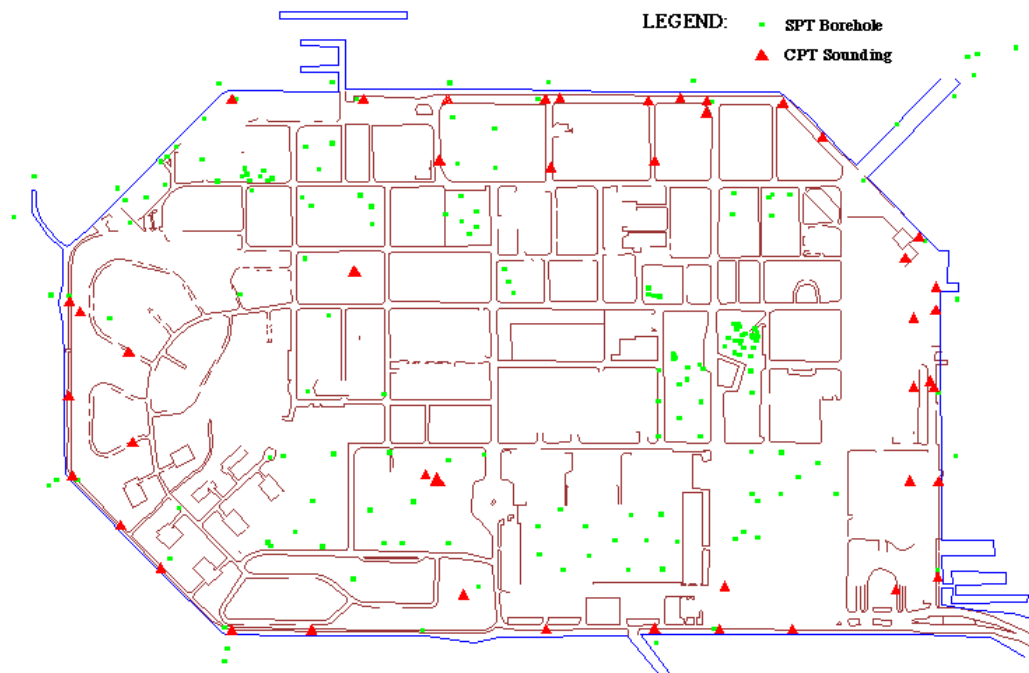


Fig. 14 - Distribution of all SPT borings and CPT soundings available in the GIS database (Luna and Frost, 1995).

form of factor of safety, cyclic stress ratio, or index). During field sampling and borehole logging, factors related to equipment and methods can affect the results. For example, the current state-of-the-practice still adheres to 2.5- or 4-inch diameter borings, however, some practices may use larger diameter boreholes. The effects of testing from relatively large boreholes in cohesive soils is probably negligible, but in sands there are indications that lower N-values may result (Skempton, 1986).

The quality of a boring log is not only dependent on the equipment and methods used in the field, but also on how the data is represented on the boring log. The depth to ground water table (DGWT) is one of the most important items in a borehole log used for liquefaction evaluation and therefore is presented in more detail as an example. If information pertaining to the DGWT measurements is not recorded, then the data set (or borehole log) is less desirable for use in a liquefaction evaluation. The fact that the DGWT was not recorded or appears blank in the borehole log does not necessarily mean that there is no ground water present. The case may be that the borehole was too shallow to encounter ground water or the borehole caved in before a measurement was made or taking the measurement was neglected. Any of these cases associated with no DGWT recorded are poor practice, but unless there is a valid entry in the borehole log it is very difficult to make an assessment of the actual DGWT. On the other hand, if there is a value for the DGWT in the boring log, it is known that an observation well (or piezometer) is more appropriate than making a DGWT measurement during the drilling process. These different cases mentioned will be associated with different levels of quality and can be accounted for quantitatively by the use of weighing factors. The data types available in the borehole log can be evaluated according to their significance in liquefaction assessment as presented for the DGWT above.

D'Andria, et al. (1995) introduced the concept of a quality attribute table that accounts for the relative importance of each data item. The quality attribute table was specifically designed for the borehole data quality evaluation for liquefaction analysis and a different table should be developed for each purpose. The method of assigning different weights or scores for each attribute found in a borehole log can be considered a way to quantify the relative quality of the logs depending on their use. This concept is very similar to the "data quality model" proposed by Venkataramanan (1996), where models were developed for different geotechnical applications including liquefaction.

At the Treasure Island pilot study site about 40 percent of the data was ignored in the development of the database since the data ranked too low in the data quality evaluation process. The spatial liquefaction analyses were run on data considered to be of medium and high quality based on the score obtained (greater than 20). This meant reducing the database used in the GIS from an original borehole log count of 300 to 178. The distribution of both SPT boreholes and CPT soundings is shown in Figure 14. A more recent study using the Treasure Island data developed a flexible hierarchical model implemented in a GIS-based application called SLOG (Deaton, et al. 2001).

Spatial Liquefaction Evaluation

When working in a GIS environment, it is important to keep in mind that such a system is principally configured for spatial analysis and database management, and thus most of the computational efforts are dedicated towards these objectives. If, in addition to the standard GIS functions, one desires to model another process, such as the liquefaction phenomenon, the additional computations cannot be mathematically complex if they are to be performed internally within the GIS. Most GIS do not support mathematical functions commonly required in engineering algorithms, although new modules are becoming available to enhance their flexibility in this area. An engineering algorithm is thus more typically programmed to operate as an add-on module while the complex spatial operations and database management functions are performed within the GIS.

To provide engineering analysis capability for the hazard system described in this paper, a well-established method, the Liquefaction Potential Index (LPI), was implemented as an operational engineering module in the GIS environment. The concept of liquefaction potential index has been presented in the literature by Iwasaki, et al., (1978) and more recently by Shinozuka (1990) and Chameau et al. (1991). The liquefaction potential index is a measure of the effect that liquefaction has on man-made structures as a function of the depth to and the extent of the liquefied zone along the vertical axis of a geotechnical exploration.

The LPI can be calculated for each sounding, as shown in the schematic in Figure 15. The term sounding is used since the data available can be in the form of a standard penetration test (SPT) or a cone penetrometer test (CPT). If the data available is in CPT form, correlations (e.g., Seed and DeAlba, 1986) can be used to convert the tip resistance (q_c) into a corrected SPT N-value [$(N_1)_{60}$]. The Seed and Idriss (1971) procedure to calculate the factor of safety for liquefaction can be performed for any depth in the soil deposit that contains a measurement of the resistance to penetration.

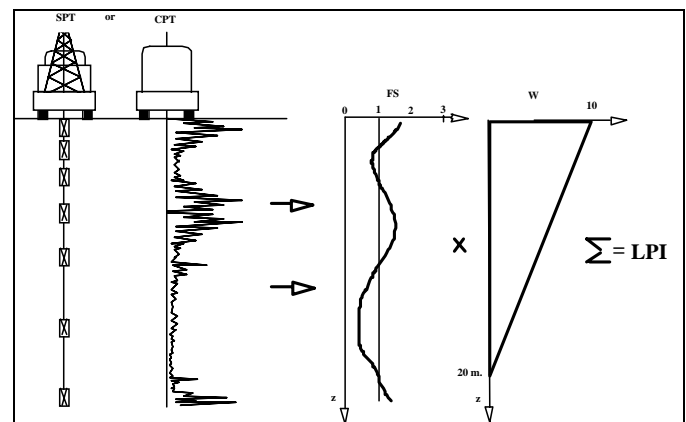


Fig. 15 - Conceptual Representation of LPI Calculation.

Once the LPI has been calculated for the soil column, this index can be compared with interval criteria that correspond to

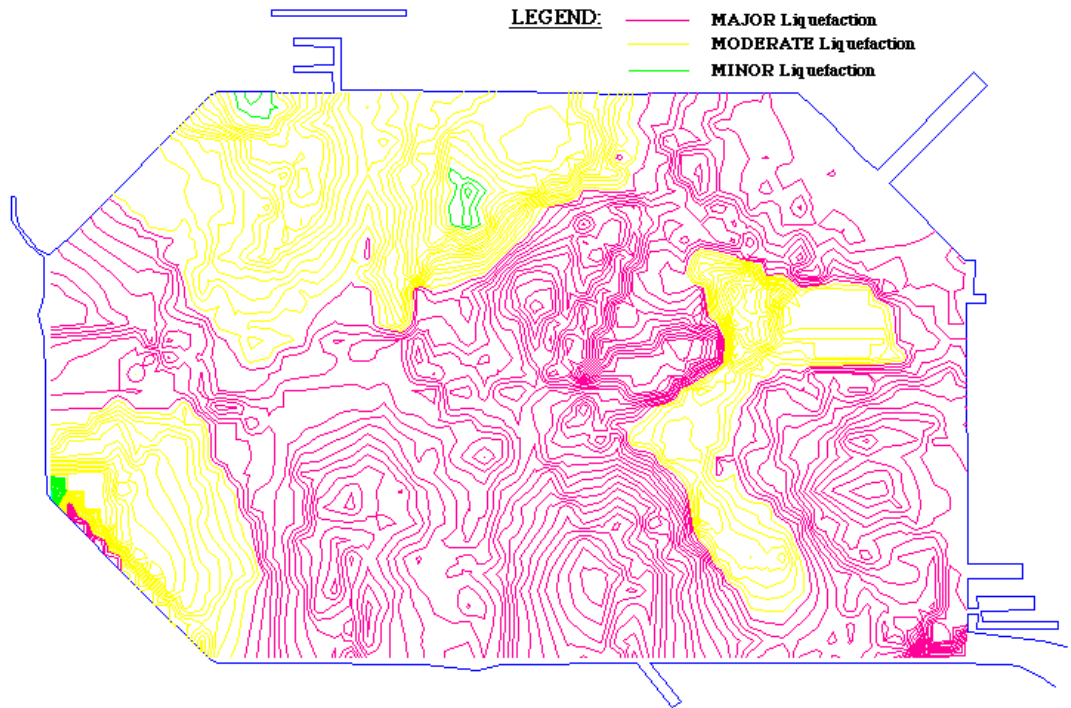


Fig. 16. LPI Contours Showing Areas with Different Liquefaction Severities for an Earthquake with $M=7.5$, $PGA = 0.3g$ using SPT Data (Luna 1995)

different levels of liquefaction. Then the index can be used to identify areas of different degrees of liquefaction. These intervals were based on a comparison of computed values of LPI with observed performance. The available intervals to date have been established by historical records of liquefaction for 85 sites in Japan (Iwasaki, 1982). Table 1 shows the proposed Japanese intervals. The LPI has not been a commonly used method in U.S. practice to date. Therefore, there have been no initiatives to collect data and evaluate liquefaction based on the LPI to develop a US based interval criteria. Nevertheless, as standard practice moves towards adopting the use of spatial analysis systems such as the one described herein, it is expected that methods such as the LPI will see increasing usage since they permit 2-D representation of 3-D phenomena through the use of the vertical weighting function.

Table 1 - LPI Intervals for Liquefaction Severity (Iwasaki, 1982)

Liquefaction Severity	LPI
Little to none	$LPI = 0$
Minor	$0 < LPI < 5$
Moderate	$5 < LPI < 15$
Major	$15 < LPI$

The initial phase of the liquefaction assessment for this site was to define the liquefaction severity criteria for the island by calculating the liquefaction potential index (LPI) in a GIS environment. The earthquake input parameters for the 1989 Loma Prieta earthquake [Magnitude (M) = 7.0 and Peak Ground Acceleration (PGA) = 0.16g] and the pre-earthquake SPT data were used to compute the LPI. The LPI criteria intervals were

varied until the Loma Prieta liquefaction conditions were obtained representing a distribution of mostly minor and moderate liquefaction contours. Also, results from previous studies (Chameau, et al., 1991) performed in the San Francisco Bay area, were used to calibrate this criteria. These results were also verified with sand boils and damage survey performed by the USGS immediately after the Loma Prieta event. Once the LPI criteria was established for this region, a number of earthquake scenarios were used in conjunction with the selected geotechnical spatial database by varying the input ground motions (magnitude and peak ground acceleration) and type of sounding.

The results of the spatial liquefaction evaluation for this site using the LPI were contoured maps developed from a grid generated with the geostatistics analysis results. The contours in their vector form can be used as a new layer of information to aid in mitigating the consequences of this hazard. For a given input acceleration and earthquake magnitude, the analyses indicate that there is spatial variability in the distribution of the liquefaction severity. The magnitude and acceleration of the earthquake was increased to an extreme event of $M = 7.5$ and peak ground acceleration of 0.3g, which resulted in a significant portion of the site subjected to liquefaction threatening the overall stability of the island (Figure 16). More detailed analyses and results are given in Luna (1995); Luna and Frost (1998).

Permanent deformations can be a result of loss of strength, flow, densification, sand boils, lateral spreading, ground rupture or a combination of these factors. Large deformations of sands during and after earthquake events are frequently the result of liquefaction. A number of procedures have been presented in the literature in the past 20 years and the error in the prediction of these deformations can be as high as 25 to 50% (Tokimatsu and Seed, 1987; Kramer, 1996). The level of complexity in these

procedures can vary from non-linear dynamic computer models (DESRA or TARA-3FL) to simplified procedures that estimate the volumetric strain based on the cyclic stress ratio and corrected SPT N-value. The time (immediate or delayed) in which these liquefaction induced deformations occur varies depending on the ability of the soil deposit to drain the pore pressure buildup generated during earthquake loading. The deformations being considered in this study pertain to the surficial evidence of volumetric strain caused during liquefaction, referred to hereafter as settlement. It is recognized that the problem of liquefaction induced deformations is a complex soil behavior phenomena, especially when the densification of a deposit (contractive behavior) is combined with the occurrence of sand boils. Sand boils may present an added degree of complexity when settlements are evaluated since the ground typically raises at the sand boil location causing even more differential settlement in a small area.

Tokimatsu and Seed (1987) reviewed available procedures and developed a simplified method of analysis to predict earthquake-induced settlement (one-dimensional) in both saturated sands and non-saturated sands. This method recognized that the primary factors controlling liquefaction-induced settlement are the cyclic stress ratio (CSR) for saturated sands with pore pressure generation and the cyclic shear strain for dry or partially saturated sands, together with the N-value or relative density, and the magnitude of the event. Using a correlation between the $(N_1)_{60}$ and relative density, and an estimate of the shear strain potential of liquefied soil from $(N_1)_{60}$ vs CSR, Seed, et al. (1984) procedure, they developed a chart (Figure 17(a)) that allows for the estimation of volumetric strain based on CSR and $(N_1)_{60}$.

More recently, Ishihara and Yoshimine (1992) developed a procedure to evaluate the volumetric strain based on the factor of safety against liquefaction and, maximum shear strain (γ_{max}) and relative density (D_r). For relative density they provide the same curve to represent other indirect forms of this parameter via

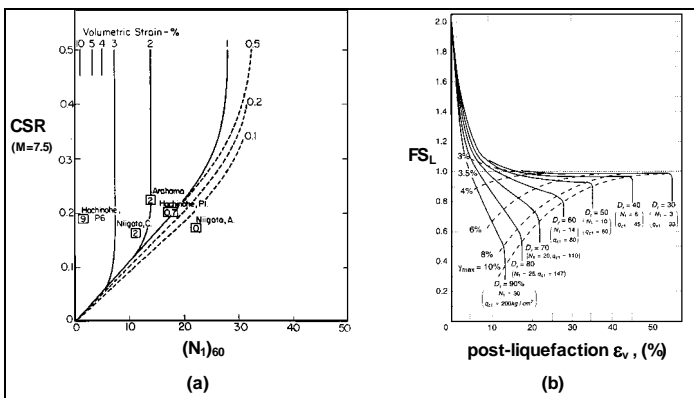


Figure 17. Charts to estimate Post-liquefaction Volumetric Strain (a) Tokimatsu and Seed (1987) and (b) Ishihara and Yoshimine (1992).

penetration tests such as N_1 , for the SPT and q_{c1} for the CPT (see Figure 17(b)).

In some cases, geotechnical design engineers are faced with the problem of a “marginal” liquefaction condition at a site that is underlain with saturated sands. This condition may be due to a relatively small earthquake event, small number of cycles of shear strain or a competent relative density, and it may be concluded that an overall foundation failure at the site due to liquefaction is not likely to occur. This condition does not exclude the possibility of liquefaction induced deformations (settlements). Tokimatsu and Seed (1987) combined earlier work presented in Tokimatsu and Yoshimine (1983) and Lee and Albaisa (1974) to develop a relationship between normalized stress ratio and volumetric strain. This relationship shows that volumetric strain is about 0.1% if the CSR ratio is 80% and insignificant if the CSR is less than 70%. Depending on the characteristics of the soil and the drainage path, the time required for all settlement to develop can vary from immediately to about a day.

Other relationships to estimate the volumetric strain have been proposed or are in development (Castro, 1987, 1991) such as direct relationships to the cyclic shear strain based on laboratory data. Other work has been adapted from the work mentioned above to be used in local practice building codes (Soydemir, 1986). The procedures mentioned in this section were selected from the literature based on their use in practice, however, the list is not exhaustive. In order to evaluate the impact of vertical settlements on existing or planned structures, it is necessary to obtain the spatial distribution across the site and analyze each type of structure using the corresponding total and differential settlement.

Spatial LIQUFAC

The US Navy developed a computer program, LIQUFAC (NAVFAC, 1994), that incorporates some of the procedures mentioned in the previous section. LIQUFAC evaluates the soil liquefaction potential for a level site. For layers which liquefy, the program estimates the one-dimensional compression settlement due to earthquake loading. This computer program follows procedures outlined in Seed, et al. (1984), Castro (1987) and NRC (1985).

LIQUFAC was designed to run in a MS-DOS environment and uses input by means of a menu driven user interface. The input subsurface soil data could be a summary of the site data or specific data from a borehole location. The earthquake characteristics are combined with the soil data to calculate a cyclic stress ratio and evaluate the potential for liquefaction using a factor of safety (FS_L). If the soil layer liquefies ($FS_L < 1.0$) then the cyclic shear strain (γ_{cyc}) as defined by Tokimatsu and Seed (1987) is calculated.

$$\gamma_{cyc} = 0.65 \frac{a_{max}}{g} \frac{\sigma_o}{G_{max}} r_d \quad (1)$$

where,

a_{max} = maximum horizontal acceleration at ground surface

σ_o = total overburden pressure
 G_{max} = shear modulus at low strain level
 r_d = stress reduction factor.

Relationships between γ_{cyc} and volumetric strain (ϵ_v) are available in different forms (Tokimatsu and Seed, 1987, Ishihara and Yoshimine, 1992 and Castro 1987, 1991) depending on the soil type, however, LIQUFAC allows the flexibility to input the data points of this relationship. Finally the one-dimensional settlement can be calculated by adding the compression in each layer.

To expand the functionality of LIQUFAC and in particular incorporate the spatial distribution of deformation in design considerations, Spatial LIQUFAC was developed (Luna, et al. 1998). The system was designed to work on a desktop PC Windows™ environment as a GIS application running under Arcview® (Environmental Systems Research Institute) and accessing a modified MS-DOS version of LIQUFAC. The customized application was programmed using an object-oriented programming language called Avenue™ that allows integration of available objects and routines in Arcview®. The original version of LIQUFAC was modified to allow control of the input data via a new GIS interface and allows for the management of the spatially distributed boreholes across the site. The program queries the borehole database and allows the user to modify the retrieved data as necessary.

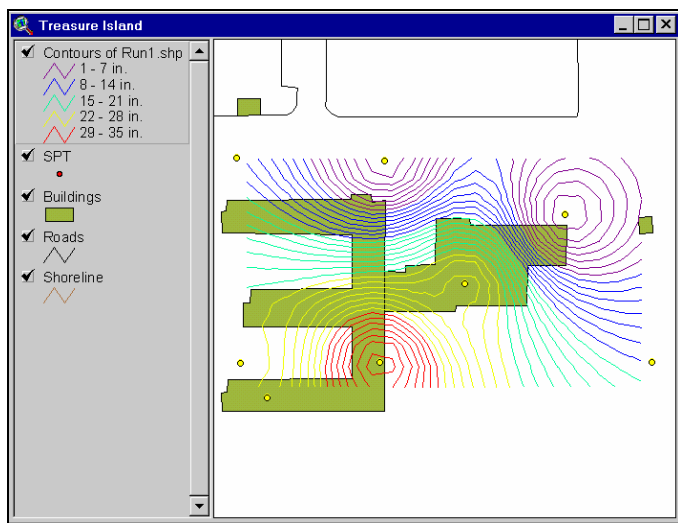


Fig. 18. Settlement distribution overlaid with building footprint (Luna, et al. 1998).

During the development of this prototype system there was a prevalent goal to make this spatial evaluation a design tool for the engineer. By bringing other layers of information in the spatial environment, such as buildings, utilities and other services, the geotechnical engineer can use this design tool to interact with other engineers designing new facilities or retrofit existing infrastructure components. An example (see Figure 18) of the output showing overlaid settlement contours and the building footprint suggest considerable differential settlement

across the structure. Future enhancements to these programs can include the use of CPT (Stark, 1995) and or shear wave velocity (Andrus, et al., 2003) data for direct calculation of liquefaction potential and deformations using recent relationships.

CASE STUDY 3:

Nisqually Earthquake Reconnaissance (Feb-Mar 2001)

On February 28, 2001 a significant earthquake ($M_w = 6.8$) occurred in the Puget Sound area of western Washington. Christened the Nisqually earthquake, this intraslab subduction zone event occurred along a high-angle normal fault, due to downdip tension in the subducting Juan de Fuca Plate. It was similar in mechanism and magnitude to the Puget Sound earthquake of April 13, 1949 ($M_w = 7.1$) and the Seattle earthquake of April 29, 1965 ($M_w = 6.7$). The hypocenter for the earthquake was located 52 km beneath the southern tip of Puget Sound, about 8 km east northeast of Olympia.

The Nisqually earthquake produced strong ground shaking over a wide area and caused noticeable damage in the Olympia, Seattle, and Tacoma areas of the Puget Lowland in Washington. No fatalities are directly attributable to the earthquake, but damage was estimated at \$2 billion (Bray, et al, 2001). Although the intensity of ground motions was not especially severe, dozens of buildings were red-tagged, and hundreds more were damaged. Observations of liquefaction were widespread in parts of Olympia and South Seattle, and several significant lateral spreads, embankment slides, and landslides occurred. The relatively long duration of the event and the relatively low cyclic resistances of some of the fills in the area are likely causes for the significant liquefaction and ground failure that was observed.

The National Science Foundation-Pacific Earthquake Engineering Research Center (NSF-PEER) funded a team from U.C. Berkeley to make a preliminary reconnaissance and post their findings on the Internet, at <http://peer.berkeley.edu/nisqually/geotech/>. The Berkeley team used hand-held GPS receivers with onsite recordation to locate themselves and each digital ground photo that was imaged. Location data were placed on an array of digital map products, including DRGs, local agency GIS maps, oblique photos and digital aerial photos. Excerpts from the web-posted report are reproduced here to give a flavor of what types of geospatial information can quickly be assembled and posted on the world wide web. The Berkeley reconnaissance focused on selected areas identified previously as having suffered ground failures with the goal of developing well-documented case histories of liquefaction and lateral spreading and their effect on engineered systems (from Bray et al., 2001 - a NSF-PEER sponsored reconnaissance effort).

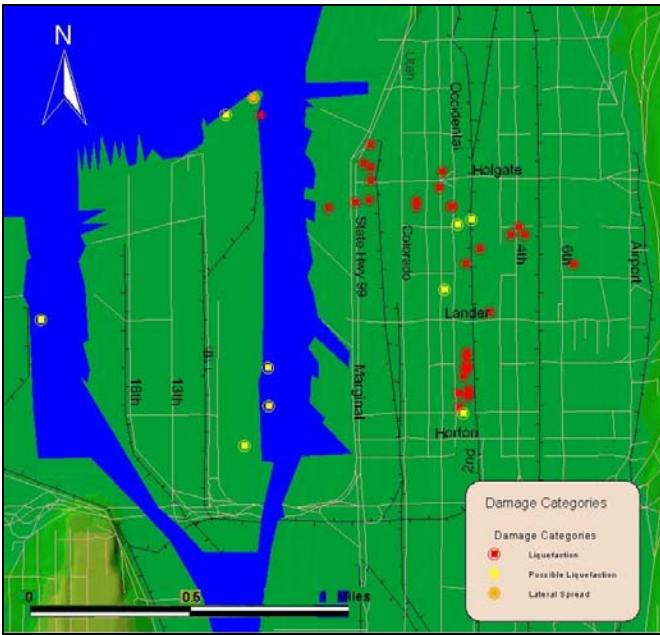


Fig. 19. Digitized street map of the South Seattle area, used to show the locations of observed liquefaction boils, located using GPS receivers. Ground photos (see below) were keyed to this map (from Bray, et al, 2001).



Fig. 20. Sand ejected from a ground fissure crossing railroad tracks at the Port of Seattle. The opening was found to run through the road into the port facilities seen in the background. All ground photos were georeferenced using GPS receivers (N47.58487° W122.33980°), (from Bray, et al, 2001).

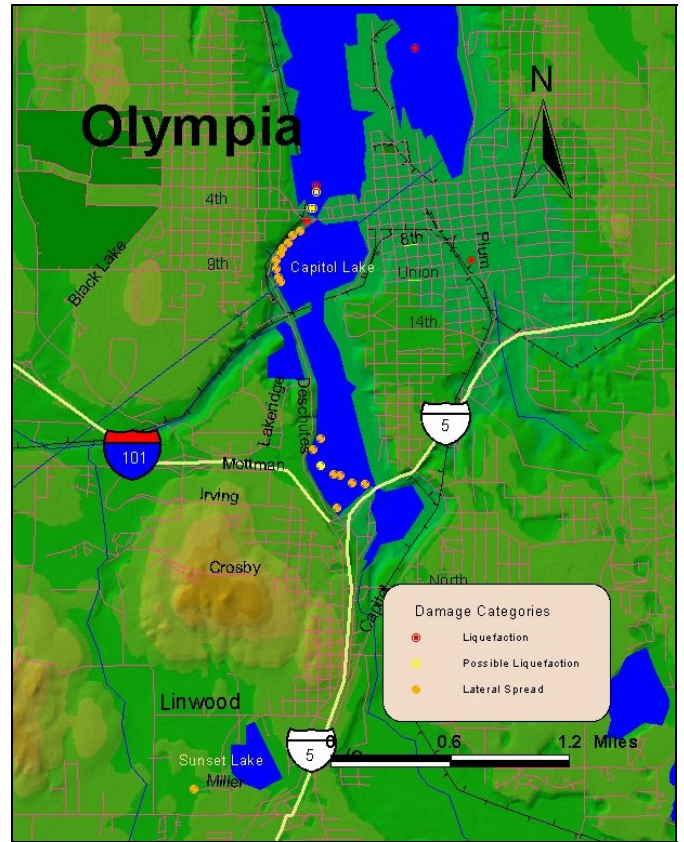


Fig. 21. Some of the observation points plotted in water on the digitized base maps provided by local agencies, in this case Thurston County, WA. These errant points were located in previously submerged areas had been reclaimed by infilling after the base map was digitized. Such discrepancies actually aided the reconnaissance team identify areas of recent filling, which were more susceptible to liquefaction (from Bray, et al, 2001).

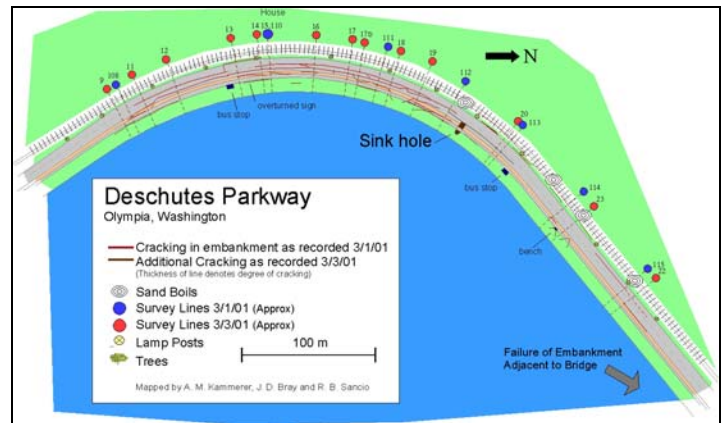


Fig. 22. Digitized assessor's parcel maps prepared by local agencies were suitable for detailed base mapping, showing locations of individual sand boils, sink holes, ground cracks and locations of photos documenting damage (from Bray, et al, 2001).



Gujarat, India earthquake (Deaton and Frost, 2002).

CASE STUDY 4:

Earthquake Shaking Intensity Maps

In 2003 the Association of San Francisco Bay Area Governments (ABAG) introduced a series of shaking intensity maps, based on the most likely earthquakes that could be generated on 18 fault segments surrounding the San Francisco Bay metropolitan area of northern California (Figure 23). These are intended to depict the general risk within neighborhoods and the relative risk of earthquake-induced shaking from community to community.

The general public can access ABAG's website at <http://www.abag.ca.gov/bayarea/eqmaps/pickcity.html> and follow their directions for viewing an earthquake shaking hazard map. Each Bay Area earthquake scenario is assumed to be caused by rupturing of a single fault or fault segment. Thus, to view an earthquake intensity map of a particular area, one simply selects an area or city of interest and then selects a nearby fault as the source of an earthquake.

Each fault is shown as a color-coded line on the map reproduced in Figure 25. The most interesting scenarios are those involving multiple fault segments on the San Andreas and Hayward faults, which tend to control the peak ground accelerations expected at any given site. Figure 26 presents the shaking intensity map for an M_w 7.2 event on the peninsula segment of the San Andreas fault, similar to the type of earthquake that occurred in 1906.

The linear nature of the shaking intensities is tied to the structural geologic grain of the San Francisco Bay region, which strikes northwesterly. Geologically young materials like alluvium and estuarine silt can amplify ground shaking through wave impedance. These are the areas that have historically suffered the greatest shaking-related damage and ground movement. The ABAG website also presents a list of *Frequently Asked Questions* that includes information on the probability of various earthquakes. The purpose of the ABAG hazard maps is to educate the public, emergency response personnel, scientists, engineers, architects and decision makers about the relative risks of ground shaking in different parts of the San Francisco Bay area.

CONCLUSIONS

GIS and remotely sensed imagery are here to stay and will continue to impact geotechnical engineering, especially in regards to how subsurface geospatial data is communicated with clients and the public at-large. Our ability to understand the complexity of a geoproblem is greatly enhanced in map form or a different graphical rendition. In the future GIS products will allow engineers to see geo-mechanisms not apparent in more traditional forms of maps and site characterization.

The use of GIS and Remote Sensing technologies is increasing rapidly and are the perfect forum for geotechnical engineers to

Fig. 23 – Example photo documenting site damage, imaged along North Deschutes Parkway showing a lateral spread toward Capitol Lake, which is to the right of the photograph. All photos were georeferenced and dated (from Bray, et al, 2001).



Fig. 24. Aerial oblique images are valuable in providing perspective and relative elevation changes that are not easily discern on vertical images. This image was pulled off the web and annotated to reflect locations where site damage was documented by the Berkeley reconnaissance team (from Bray, et al, 2001).

The widespread availability of digitized base maps, USGS topographic quadrangles and digital orthophotos in combination with hand-held GPS receivers and palm pilots allows accurate recording of perishable data, which can prove of inestimable value later. Digitized maps can also provide valuable clues about past land usage and insights as to which areas were recently filled, as shown in Figure 21. Hand held GPS receivers with data storage receptacles can also be used to construct new maps, based on the paths traversed during any reconnaissance. A new handheld palm top application PQUAKE is available for the reconnaissance of earthquakes and was used in the recent 2001

work more closely with other geo-professionals. Importance needs to be placed on the different levels of quality that we associate the various types of geotechnical data, some of the progress that has been made in representations of borehole data are reported herein. Aerial and remotely sensed imagery is becoming more accessible to the geotechnical engineer and when it is registered to geographic coordinates and used in combination with other line and point data, it dramatically enhances our interpretation of the geoproblem. Hyperspectral imagery is currently being used in geo-engineering by only a few due to the scarce availability of commercial data, but in this information age it will soon be available over the Internet and will be becoming increasingly commonplace.

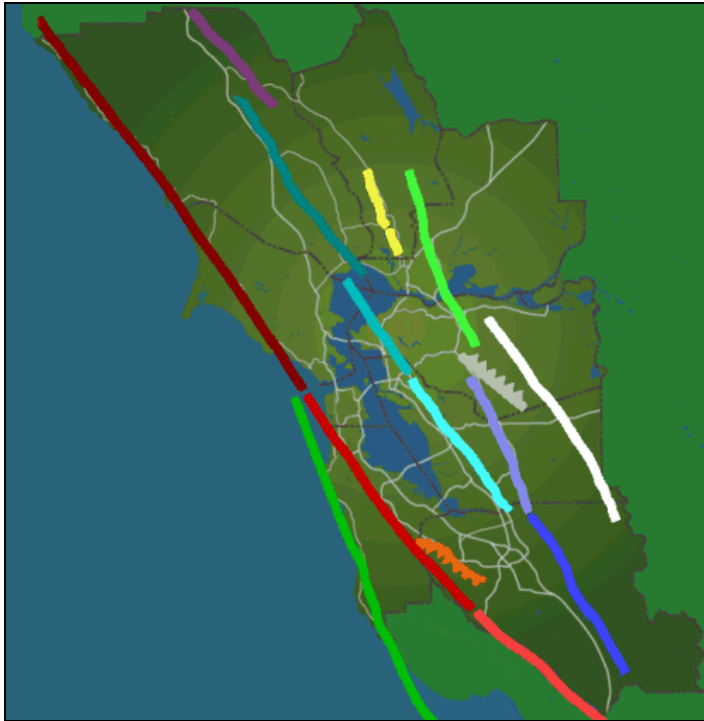


Fig. 25. Earthquake fault source map displayed on ABAG's web site. The active fault segments are color-coded and listed on a table.

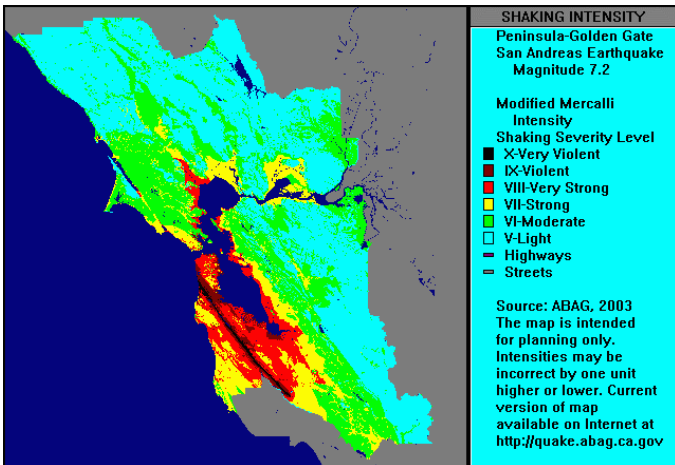


Fig. 26. Predicted earthquake shaking intensity map for M_w 7.2 quake on peninsula segment of the San Andreas fault in the San Francisco Bay area.

REFERENCES

- Andrus, R., Stokoe, K., Chung, R., and Juang, C., (2003), "Guidelines for Evaluating Liquefaction Resistance using Shear Wave Velocity Measurement and Simplified Procedures", Report No. NIST GCR 03-854, National Institute of Standards and Technology, Gaithersburg, MD, 151 pp.
- Association for Planning and Regional Reconstruction, 1950, *Town and Country Planning Textbook*: Architectural Press, London, 613 p.
- Bradnt, A., 1990, Sherman Fairchild Looks at the World: *Air & Space Smithsonian*, v.4: 4 (November), pp. 96-99.
- Bray, J.D., Sancio, R.B., Kammerer, A.M., Merry, S., Rodriguez-Marek, A., Khazai, B., Chang, S., Bastani, A., Collins, B., Hausler, E., Dreger, D., Perkins, W.J., and Nykamp, M., 2001, *Some Observations of Geotechnical Aspects of the February 28, 2001 Nisqually Earthquake in Olympia, South Seattle, and Tacoma, Washington*: On-line at <http://peer.berkeley.edu/nisqually/geotech/>
- Castro, G. (1987), "On the Behavior of Soil During Earthquake-Liquefaction," in *Developments in Geotechnical Engineering 42, Soil Dynamics and Liquefaction*, Edited by Cakmak, A.S., Elsevier, pp. 169-204.
- Chameau, J.L., Clough, G.W., Reyna, F.A. and Frost, J.D. (1991), "Liquefaction Response of San Francisco Bayshore Fills", *Bulletin of Seismological Society of America*, Vol. 81, No. 5, pp. 1998-2018.
- D'Andria, G., J.D. Frost, R. Luna, and E.J. Macari (1995), "Quality of Borings for Use in Liquefaction Spatial Analysis", *Proc. of the 10th PanAmerican Conference on Soil Mechanics and Foundation Engineering, Guadalajara, Mexico*, Vol 3, pp. 1739-1749.
- Deaton, S.L., and Frost, J.D., (2002), "Integrated Digital Earthquake Reconnaissance", 7th U.S. National Conference on Earthquake Engineering, CD-ROM.
- Deaton, S.L., Frost, J.D., Luna, R., and Parsons, R.L., (2001), "GIS-Based Evaluation of Geotechnical Borehole Log Quality", *Journal of the Transportation Research Board*, TRR No. 1755, TRB/NRC, Washington, D.C., pp. 15-25.
- Estes, J.E., Jensen, J.R. and Simonett, D.S., 1980 *Impacts of Remote Sensing on U.S. Geography: Remote Sensing of Environment*, v. 10:43- 80.
- Geolith, Inc., 2000, *Mission Peak Landslide, Fremont, California*: consultant's report to City of Fremont; three vols., Executive Summary, (v. 1), 15 p., 6 figs, 45 pl.; Technical Report (v. 2), 82 p., 47 figs, 5 pl.; and Technical Data (v. 3), 87 figs.

- Geomatrix Consultants (1990), "Evaluation of Interior Area Performance - Naval Station Treasure Island, San Francisco, California", Report prepared for Western Division NAVFAC, Vols. 1, 2, 4, 5, Geomatrix Consultants, October.
- Haugerud, R.A., Harding, D.J., Johnson, S.Y., Harless, J.L., Weaver, C.S., and Sherrod, B.L., 2003, High-Resolution Lidar Topography of the Puget Lowland, Washington – A Bonanza for Earth Science: *GSA Today*, v. 13:6 (June), p. 4-10.
- Ishihara, K. and Yoshimine, F. (1992), "Evaluation of Settlements in a Sand Deposit Following Liquefaction during Earthquakes," *Soils and Foundations*, JSSMFE, Vol. 32, No. 1, pp. 173-188.
- Iwasaki, T., Tatsuoka, F., Tokida, K. and Yasuda, S. (1978), "Estimation Procedure of Liquefaction Potential and its Application to Earthquake Resistance Design", U.S.-Japan Panel on Wind and Seismic Effects, UJNR, 22 pp.
- Iwasaki, T., Tokida, K., Tatsuoka, F., Watanabe, S., Yasuda, S. and Sato, H. (1982), "Microzonation for Soil Liquefaction Potential Using Simplified Method", *Proc. of the 3rd International Earthquake Microzonation Conference*, Seattle, pp. 1319-1330.
- Jurasius, M., 2002, *Rock Slope Kinematics of the Mission Peak Landslide, Fremont, CA*: M.S. thesis in geology: San Jose State University, 167 p.
- Kiremidjian, A.S., (1997), "Spatial Analysis in Geotechnical Earthquake Engineering", ASCE, *Geotechnical Special Publication*, No. 67, pp. 1-14.
- Kramer, S.L., (1996), "Geotechnical Earthquake Engineering", Prentice Hall, New Jersey, 453 pp.
- LaHusen, R.G., and Reid, M. E., 2000, A Versatile GPS System for Monitoring Deformation of Active Landslides and Volcanoes: *Transactions of the American Geophysical Union*, v.81, n.48, p.F320.
- Lee, K.L. and Albasia, A. (1974), "Earthquake Induced Settlements in Saturated Sands", *Journal of the Soil Mechanics and Foundations Division*, ASCE, Vol. 100, No. GT4, pp. 387-400.
- Lisaewski, M., 2003, The Grand Canyon's Landmark Map Dataset: *Geospatial Solutions*, v.13:3, pp. 26-30.
- Luna, R. (1995), "Liquefaction Evaluation Using a Spatial Analysis System", Ph.D. Thesis, School of Civil and Environmental Engineering, Georgia Institute of Technology, Atlanta, GA.
- Luna, R. and Frost, J.D., (1998), "Spatial Liquefaction Analysis System", *Journal of Computing in Civil Engineering*, ASCE, Vol. 12, No. 1, pp. 48-56.
- Luna, R., Carroll, D., Frost, J.D., and Wu, A., (1998), "Spatial Evaluation of Earthquake Induced Deformations", ASCE, *Geotechnical Special Publication*, No. 75, pp. 398-409.
- McHarg, I. L., 1969, *Design with Nature*, American Museum of Natural History, Garden City, New York, 198 p.
- Miles, S.B. and Ho, C.L., (1999), "Applications and Issues of GIS as a Tool for Civil Engineering Modeling", *Journal of Computing in Civil Engineering*, ASCE, Vol. 13, No. 3, pp. 144-152.
- NAVFAC (1994), "Liquefaction Potential Analysis - LIQUFAC User Documentation", Naval Facilities Engineering Command, report prepared by Information Dynamics, Inc., 58 pp.
- NRC, National Research Council, (1985), "Liquefaction Soil During Earthquakes", National Academy Press, Washington, D.C., 240 pp.
- Rogers, J. D. and Drumm, P.L., 1999, *Overview of the 1998 Mission Peak Landslide, Fremont, California: Field Trip Guide*, Northern California Geological Society, May 8, 1999, 27p., 1pl.
- Seed, H.B., and DeAlba, P., (1986), "The Use of SPT and CPT Tests for Evaluating the Liquefaction Resistance of Sands", Use of In-Situ Tests in Geotechnical Engineering, *Geotechnical Special Publication No. 6*, ASCE, pp. 291-302.
- Seed, H.B., and Idriss, I.M., (1971), "Simplified Procedure for Evaluating Soil Liquefaction Potential", *Journal of Soil Mechanics and Foundations Division*, ASCE 97(SM9), pp. 1249-1273.
- Seed, H.B., Tokimatsu, K., and Harder, L.F., (1984), "The Influence of SPT Procedures in Soil Liquefaction Resistance Evaluation", Report No. UBC/EERC-84-15, Earthquake Engineering Research Center, University of California, Berkeley.
- Shinozuka, M., (1990), "Crude Oil Transmission Study - Probabilistic Models for Liquefaction", *NCEER Bulletin*, October, pp. 3-8.
- Skempton, A. W., 1986, "Standard Penetration Test Procedures and the Effects in Sands of Overburden Pressure, Relative Density, Particle Size, Aging, and Overconsolidation", *Geotechnique*, 36, No. 3, pp. 425-447.
- Soydemir, C., (1986), "Seismically Induced Settlements: Two Models for New England", *Proceedings of the Third U.S. National Conference on Earthquake Engineering*, Charleston, S.C., Vol I, pp. 565-573.
- Star, Jeffrey and Estes, John, 1990, *Geographic Information Systems: An Introduction*, Prentice-Hall Canada, Scarborough, ON, Canada, 303 p.
- TC4, (1993), Technical Committee for Earthquake Geotechnical Engineering, *Manual for Zonation on Seismic Geotechnical Hazards*, ISSMFE, 149 pp.
- Tokimatsu, K. and Seed, H.B., (1987), "Evaluation of Settlement in Sands due to Earthquake Shaking", *Journal of Geotechnical Engineering*, ASCE, Vol. 113, No. 8, pp. 861-878.
- Tokimatsu, K. and Yoshimine, Y., (1983), "Empirical Correlation of Soil Liquefaction based on SPT N-value and fines content", *Soils and Foundations*, JSSMFE, Vol. 21, No. 3, pp. 56-74.

Venkataramanan, C. (1996). "A System for Data Quality Evaluation Applied to Borehole Logs", M.S. Thesis, School of Civil and Environmental Engineering, Georgia Institute of Technology. Atlanta, Georgia. pp.1-108.